

COMETA-2026-05

Is the Standard Model Effective Field Theory Enough for Higgs Pair Production?

Íñigo Asiáin^{*1}, Ramona Gröber^{†2}, and Lorenzo Tiberi ^{‡3}

¹*Departament de Física Quantica i Astrofísica, Institut de Ciències del Cosmos (ICCUB), Universitat de Barcelona, Martí Franquès 1, 08028 Barcelona, Spain*

²*Dipartimento di Fisica e Astronomia “G. Galilei”, Università di Padova, and Istituto Nazionale di Fisica Nucleare, Sezione di Padova, I-35131 Padova, Italy*

³*Dipartimento di Fisica e Geologia, Università di Perugia, and Istituto Nazionale di Fisica Nucleare, Sezione di Perugia, I-06123 Perugia, Italy*

Abstract

We study Higgs-boson pair production in the Standard Model Effective Field Theory (SMEFT) up to dimension six and in the Higgs Effective Field Theory (HEFT) at leading order in the effective theory expansion, and assess which description is appropriate in concrete UV scenarios. Motivated by “Loryon”-inspired models, we compare the Higgs pair production cross sections predicted by the full models to their SMEFT and HEFT counterparts. We identify regimes in which the two EFTs provide comparable descriptions, and clarify the limits required for their couplings to match. We also find that, for parts of parameter space in some of these models, HEFT can reproduce Higgs pair production more accurately than SMEFT, highlighting di-Higgs measurements as a potential probe of non-linear electroweak dynamics.

^{*}iasiain@icc.ub.edu

[†]ramona.groeber@pd.infn.it

[‡]lorenzo.tiberi@dottorandi.unipg.it

1 Introduction

After the discovery of the Higgs boson in 2012 [1, 2], huge progress has been made in its characterisation [3, 4]. So far no significant deviation with respect to the Standard Model (SM) predictions has been found, neither by coupling measurements of the Higgs boson nor by direct searches for new physics. This motivates an effective field theory (EFT) approach that can be used to parameterise new physics effects in a model-independent way.

The two candidate EFTs are the Standard Model Effective Field Theory (SMEFT) [5–7] and Higgs Effective Field Theory (HEFT) also known as electroweak chiral Lagrangian [8–14]. They distinguish themselves on the assumptions made on the Higgs field as well as on the counting used for the ordering of the effective operators [15–17]. In SMEFT, the Higgs field transforms as an $SU(2)$ doublet as in the SM, while in HEFT the physical Higgs boson transforms as a singlet under the SM gauge group. In SMEFT the operators are ordered by their canonical dimension, whereas in HEFT a chiral dimension counting can be adopted [16, 17].

Recent years have seen substantial progress in clarifying when HEFT, rather than SMEFT, provides the appropriate low-energy description. More precisely, although the Higgs and Goldstone degrees of freedom can always be assembled into an $SU(2)$ doublet H , HEFT is required when the effective Lagrangian cannot be written as an analytic expansion around $H^\dagger H = 0$, up to field redefinitions [18]. In Refs. [19–22] this criterion has been given a geometric interpretation: treating the Higgs and Goldstones as coordinates on a Riemannian scalar manifold, HEFT is needed when the scalar manifold has no fixed point of the $O(4)$ symmetry. A more phenomenological viewpoint was advocated in [23, 24], where the necessity of HEFT over SMEFT was linked to the presence of zeros in the flare function.

Clearly, HEFT is more general than SMEFT [25] and generically predicts larger deviations with a validity of the framework up to a scale of $4\pi v$ where v is the vacuum expectation value of the scalar field. While in the SMEFT the SM limit can be achieved smoothly by setting the scale that suppresses the operators of higher dimensions to large values, in the HEFT the SM limit is obtained by tuning the coefficients in front of the operators to one or zero.

In this paper, we will study from a phenomenological point of view whether it will be necessary to adopt the more general HEFT for studies in Higgs pair production or whether it is sufficient to describe potential deviations in terms of SMEFT by adopting concrete UV scenarios and connecting them to HEFT and SMEFT.

While Higgs pair production is usually considered a probe of the trilinear Higgs self-coupling [26–28], it can also be used to probe *Higgs non-linearities* [29–31] hence whether the couplings of one or several Higgs bosons are connect via the linear EFT relations given in SMEFT. In particular in Higgs pair production in vector boson fusion, one can directly probe the *flare* function that distinguishes between HEFT and SMEFT in the two-derivative case [23, 24, 32]. This is due to the fact that in SMEFT couplings of one Higgs boson to vector bosons, gluons and fermions are usually correlated with the equivalent coupling to two Higgs bosons at the same order in the EFT expansion, while in the HEFT they are not correlated. We notice though that, as has been shown recently in [33] for Higgs pair production in gluon fusion, that this is purely a question about which EFT converges faster. For this reason, we stay at the order in the EFTs commonly adopted in current experimental

analyses – LO HEFT Lagrangian and dimension six in SMEFT.

The couplings of two Higgs boson to fermions or vector bosons are already probed by the ATLAS and CMS experiments [34, 35]. One of the questions we assessed in this work, is whether the current bounds on these kind of couplings probe realistic parameter space in terms of concrete models.

In a first step, we identify candidate UV scenarios in which the appropriate low-energy description is HEFT rather than SMEFT. A well-defined class of such models was introduced in Ref. [36] under the name Loryons, building on the criterion of Ref. [22]: the new states should acquire more than half of their mass from electroweak symmetry breaking. When this condition is met, the SMEFT expansion is not the natural organizing principle and a HEFT description is required. Phenomenological studies of Loryons include, for instance, Refs. [37, 38]. In our analysis we select representative Loryon setups and augment their Lagrangians with additional interactions that generate tree-level matching coefficients, thereby enhancing their impact on Higgs pair production. More generally, HEFT can also be necessitated by scenarios with additional sources of electroweak symmetry breaking [22].

For three benchmark models – the singlet extension of the SM, the two-Higgs-doublet model, and a colored-scalar extension – we compute their contributions to Higgs pair production in the UV theory and compare them to the corresponding descriptions in SMEFT and HEFT. This allows us to delineate in a concrete way when HEFT is required, and when SMEFT remains sufficient, for interpreting Higgs-pair searches. Related questions have been explored for Higgs pair production in vector boson fusion in Ref. [39].

The paper is structured as follows. In section 2 we discuss the two different EFT parameterisations of Higgs pair production. In section 3 we first discuss how we identify the considered models and then discuss them one by one. We offer our conclusions in section 4.

2 Effective Field Theory Description of Higgs pair production

A Higgs boson pair is dominantly produced in the SM by gluon fusion. The cross section is around 37 fb at $\sqrt{s} = 14$ TeV [40–46]. The second most important Higgs pair production process is vector boson fusion (VBF) with a cross section of 2 fb at $\sqrt{s} = 14$ TeV [28, 47–49]. In effective field theory descriptions those two processes receive modified couplings as well as new structures from effective operators. We define the SM Lagrangian as

$$\mathcal{L} = (D_\mu H)^\dagger (D^\mu H) - V(H) - \frac{1}{4} B_{\mu\nu} B^{\mu\nu} - \frac{1}{4} W_{\mu\nu}^a W^{\mu\nu,a} - \frac{1}{4} G_{\mu\nu}^a G^{\mu\nu,a} - \left(y_d \bar{q}_L H d_R + y_u \bar{q}_L \tilde{H} u_R + y_e \bar{\ell}_L H e_R + \text{h.c.} \right) + \sum_{\psi=q_L,\ell_L,u_R,d_R,e_R} i \bar{\psi} \not{D} \psi, \quad (1)$$

with $\tilde{H}_i = \epsilon_{ij} H_j$, the ℓ_L and q_L are the $SU(2)_L$ lepton and quark doublets, e_R, d_R, u_R the $SU(2)_L$ singlets, $B_{\mu\nu}, W_{\mu\nu}, G_{\mu\nu}$ the $U(1)$, $SU(2)$ and $SU(3)$ field strengths and the Higgs potential is given by

$$V(H) = \mu_1^2 |H|^2 + \lambda_H |H|^4, \quad (2)$$

with H the scalar doublet field, taking the form $H = 1/\sqrt{2}(0, v_H + h)^T$ in the unitary gauge. For our considerations the following SMEFT operators are relevant (using the so-called Warsaw basis [6])

$$\begin{aligned} \Delta\mathcal{L}_{\text{SMEFT}} = & \frac{C_{H,\square}}{\Lambda^2}(H^\dagger H)\square(H^\dagger H) + \frac{C_{HD}}{\Lambda^2}(H^\dagger D_\mu H)^*(H^\dagger D^\mu H) + \frac{C_H}{\Lambda^2}(H^\dagger H)^3 \\ & + \left(\frac{C_{tH}}{\Lambda^2}H^\dagger H\bar{Q}_L\tilde{H}t_R + h.c. \right) + \frac{C_{HG}}{\Lambda^2}H^\dagger HG_{\mu\nu}^aG^{\mu\nu,a}, \end{aligned} \quad (3)$$

where Q_L stands for the third generation quark doublet. The operators $\mathcal{O}_{H,\square}$, \mathcal{O}_{HD} and \mathcal{O}_H modify Higgs pair production via gluon fusion and vector boson fusion, while all the operators of Eq. (3) affect Higgs pair production in gluon fusion. We do not explicitly write down operators that affect the light quark couplings to the Higgs boson as their importance depends on the flavour structure assumed, note though that they can be also be potentially probed in Higgs pair production [50–53]. We assume CP-conservation and refer to [54] for a study of CP-violating couplings in Higgs pair production. Furthermore, we omit operators of type $H^\dagger HW_{\mu\nu}W^{\mu\nu}$ or $(\bar{Q}_L\sigma^{\mu\nu}T^At_R)\tilde{H}G_{\mu\nu}^A$ adopting a loop counting [55, 56]. The chromomagnetic operator enters into one-loop diagrams but is loop-generated, hence counts effectively as a two-loop contribution. When adopting the loop counting it enters consistently at the same order as e.g. four-top operators [57, 58]. The operator \mathcal{O}_{HG} is also loop-generated but entering in tree-level diagrams in gluon fusion respects the considered order. As was pointed out in Ref. [59], it is useful to extract from the operator \mathcal{O}_{HG} a factor $\alpha_s(\mu)$

$$C_{HG} \rightarrow \tilde{C}_{HG} = \frac{1}{\alpha_s(\mu)}C_{HG}, \quad (4)$$

since α_s is usually evaluated at a dynamical scale in Higgs pair production via gluon fusion.

The Warsaw basis is constructed such that derivative operators are systematically removed by equations of motion, but two derivative Higgs interactions remain. Since they contain covariant derivatives they cannot be removed by gauge-independent field redefinitions. In order to obtain a canonically normalised Higgs kinetic term, the standard field redefinition (in unitary gauge) is

$$H = \frac{1}{\sqrt{2}} \left(h(1 + v^2 \frac{C_{H,\text{kin}}}{\Lambda^2}) + v \right) \quad (5)$$

with

$$C_{H,\text{kin}} = \left(C_{H,\square} - \frac{1}{4}C_{HD} \right). \quad (6)$$

In Higgs pair production it turns out to often be convenient to adopt yet another field redefinition which removes derivative Higgs self-interactions

$$h \rightarrow h + v^2 \frac{C_{H,\text{kin}}}{\Lambda^2} \left(h + \frac{h^2}{v} + \frac{h^3}{3v^2} \right). \quad (7)$$

In this way, the Higgs trilinear self-coupling gets modified by a multiplicative factor only with respect to the SM and no new derivative structures come into play. On the other hand,

it leads to a dependence on $C_{H,\text{kin}}$ for all Higgs boson couplings. In the following, we will use the field redefinition of Eq. (7).

We turn now to discuss HEFT. In that case, there is no longer a Higgs doublet structure H but the Goldstone bosons π^i , which are associated to the breaking of the $SU(2)_L \times U(1)_Y \rightarrow U(1)_Q$ can be described by the matrix

$$\Sigma = e^{i\sigma^i \pi^i/v} \quad \text{with} \quad v = 246 \text{ GeV} \quad \text{and} \quad i = 1, 2, 3. \quad (8)$$

The physical Higgs field h arises as a singlet. The relevant Lagrangian for our purpose is given by

$$\begin{aligned} \Delta\mathcal{L}_{\text{HEFT}} = & \frac{v^2}{4} \text{Tr} \left(D_\mu \Sigma^\dagger D^\mu \Sigma \right) \left(1 + 2c_{hVV} \frac{h}{v} + c_{hhVV} \frac{h^2}{v^2} \right) - m_t \left(c_t \frac{h}{v} + c_{2t} \frac{h^2}{v^2} \right) \bar{t}t \\ & - c_{hhh} \frac{m_h^2}{2v} h^3 + \frac{\alpha_s}{8\pi} \left(c_{ggh} \frac{h}{v} + c_{gghh} \frac{h^2}{v^2} \right) G_{\mu\nu}^a G^{a,\mu\nu}. \end{aligned} \quad (9)$$

We note that the operators with coefficients c_{ggh} and c_{gghh} contribute an order higher in the chiral counting¹ with respect to the other terms, but they arise at the same order once inserted into Feynman diagrams since they generate tree-level diagrams [60]. The relevant couplings for Higgs pair production are given in Table 1. We can see that HEFT provides the more general description than SMEFT. In SMEFT at dimension 6, the couplings of two Higgs boson and one Higgs boson to bosons or fermions are correlated, while they are not in HEFT. There, the couplings to two or more Higgs boson arise at the same order as the coupling of one Higgs boson as the Higgs boson does not carry chiral dimension. Of course also in SMEFT the couplings of one or two Higgs bosons to bosons or fermions can become decorrelated, but this requires to go to operators of higher dimensions. For instance at dimension 8 an operator $|H|^4 G_{\mu\nu} G^{\mu\nu}$ is part of the dimension-8 Lagrangian, decorrelating the one Higgs to gluon and the two Higgs to gluon coupling. In this case, there is however a suppression of the decorrelation effect by $1/\Lambda^2$. We refer to [61] for a study of dimension-8 effects in Higgs pair production in gluon fusion and to [62] in vector boson fusion. Higher order effects in HEFT have been considered in [63] for vector boson fusion and we refer to [60] for gluon fusion HEFT Higgs pair production including also operators beyond the LO Lagrangian.

3 UV Models

In order to answer the question whether it is sufficient to adopt SMEFT in Higgs pair production or whether HEFT should be used, we study three UV models, which are inspired by the *Loryon* catalogue [36]. We chose as examples a model that generates via tree-level matching contributions to $C_{H,\text{kin}}$ and hence a rescaling to all Higgs couplings – the singlet scalar model. With respect to [36] we do not impose a \mathbb{Z}_2 symmetry to allow for larger effects. For this case we study both Higgs pair production in gluon fusion and vector boson fusion. Then, we move to a model where the main effect can come from Higgs couplings

¹Counting also the orders of g_s into the chiral dimension [17].

HEFT	SMEFT
c_{hVV}	$1 + \frac{C_{H,\text{kin}} v^2}{\Lambda^2}$
c_{hhVV}	$1 + \frac{4C_{H,\text{kin}} v^2}{\Lambda^2}$
c_{hhh}	$1 - \frac{2v^2}{m_h^2} \frac{v^2 C_H}{\Lambda^2} + 3 \frac{v^2}{\Lambda^2} C_{H,\text{kin}}$
c_t	$1 - \frac{v^2}{\sqrt{2}\Lambda^2} \frac{v}{m_t} C_{uH} + \frac{v^2}{\Lambda^2} C_{H,\text{kin}}$
c_{2t}	$-\frac{3v^2}{2\sqrt{2}\Lambda^2} \frac{v}{m_t} C_{uH} + \frac{v^2}{\Lambda^2} C_{H,\text{kin}}$
c_{ggh}	$\frac{8\pi}{\alpha_s} \frac{v^2}{\Lambda^2} C_{HG}$
c_{gghh}	$\frac{4\pi}{\alpha_s} \frac{v^2}{\Lambda^2} C_{HG}$

Table 1: Relevant couplings in di-Higgs production.

to top quarks – the two Higgs doublet model (2HDM). The latter has been studied in the context of *Loryons* in [38]. We focus our study to gluon fusion for this model. What regards vector boson fusion, we refer to the study in [64]. Finally, we discuss a model whose leading effects are in the Higgs gluon couplings – a model featuring colored scalars.

3.1 Scalar Singlet Model

We started with the scalar singlet model. The SM is augmented with an additional real scalar field Φ . The potential then takes the following form

$$V(H, \Phi) = \mu_1^2 |H|^2 + \lambda_H |H|^4 + \frac{1}{2} \mu_2^2 \Phi^2 + \mu_4 |H|^2 \Phi + \frac{1}{2} \lambda_3 |H|^2 \Phi^2 + \frac{1}{3} \mu_3 \Phi^3 + \frac{1}{4} \lambda_2 \Phi^4. \quad (10)$$

A tadpole term for the singlet field has been omitted, as it can be reabsorbed in the singlet vacuum expectation value by a field redefinition.

The term with the μ_4 coupling unavoidably induces a vacuum expectation value for Φ and also leads to a mixing between H and Φ . On the other hand it also leads to tree-level generated effective operators for the singlet model. The potential becomes \mathbb{Z}_2 symmetric if $\mu_4 = \mu_3 = 0$. We consider here though the more general case where they are free parameters.

The scalar fields can be expanded around their vacuum expectation values by

$$H = \frac{1}{\sqrt{2}} \begin{pmatrix} 0 \\ v_H + h \end{pmatrix}, \quad \Phi = (v_S + S), \quad (11)$$

employing the unitary gauge for the Higgs doublet.

The tadpole conditions are given by

$$-\mu_4 v_S - \frac{\lambda_3 v_S^2}{2} - \mu_1^2 - \lambda_H v_H^2 = 0, \quad (12)$$

$$-\frac{\mu_4 v_H^2}{2} - \frac{1}{2} \lambda_3 v_H^2 v_S - \mu_2^2 v_S - \lambda_2 v_S^3 - \mu_3 v_S^2 = 0. \quad (13)$$

With the first condition one can replace μ_1^2 in terms of v_H . The mass terms can be diagonalised by rotation with a matrix

$$\begin{pmatrix} h_1 \\ h_2 \end{pmatrix} = \begin{pmatrix} \cos \theta & \sin \theta \\ -\sin \theta & \cos \theta \end{pmatrix} \begin{pmatrix} h \\ S \end{pmatrix}, \quad (14)$$

such that the mass matrix M^2 becomes diagonal.

The mass matrix in the real (h, S) basis then reads

$$M^2 = \begin{pmatrix} m_{hh} & m_{hS} \\ m_{hS} & m_{SS} \end{pmatrix}, \quad (15)$$

with

$$m_{hh} = 2v_H^2 \lambda_H, \quad (16)$$

$$m_{hS} = v_H (\mu_4 + \lambda_3 v_S), \quad (17)$$

$$m_{SS} = \mu_2^2 + \frac{1}{2} (\lambda_3 v_H^2 + 6v_S^2 \lambda_2 + 4v_S \mu_3), \quad (18)$$

and the mass eigenvalues are

$$\begin{aligned} m_{1,2}^2 &= \frac{1}{2} \left(m_{hh} + m_{SS} \mp \sqrt{4m_{hS}^2 + (m_{hh} - m_{SS})^2} \right) \\ &= \frac{1}{2} \left(m_{hh} + m_{SS} \pm (m_{hh} - m_{SS}) \frac{1}{\cos 2\theta} \right). \end{aligned} \quad (19)$$

The mixing angle θ is given by the relation

$$\tan 2\theta = \frac{2m_{hS}}{m_{SS} - m_{hh}}. \quad (20)$$

We can treat now some of the potential parameters in terms of the masses m_1 and m_2 , the

vacuum expectation values v_H and v_S as well as the mixing angle θ via the following relations

$$\mu_1^2 = -\frac{1}{4} \left[(-2\lambda_3 v_S^2 + m_1^2 + m_2^2) + \cos 2\theta (m_1^2 - m_2^2) - 2\frac{v_S}{v_H} \sin 2\theta (m_1^2 - m_2^2) \right], \quad (21)$$

$$\mu_2^2 = \frac{1}{2} \left[(\lambda_3 v_H^2 - m_1^2 - m_2^2 + 2\lambda_2 v_S^2) + \frac{v_H}{v_S} \sin 2\theta (m_1^2 - m_2^2) + \cos 2\theta (m_1^2 - m_2^2) \right], \quad (22)$$

$$\begin{aligned} \mu_3 &= \frac{1}{2v_S} (m_1^2 + m_2^2 - \lambda_3 v_H^2 - 4\lambda_2 v_S^2) - \frac{1}{4} \frac{v_H}{v_S^2} \sin 2\theta (m_1^2 - m_2^2) \\ &\quad - \frac{1}{2v_S} \cos 2\theta (m_1^2 - m_2^2), \end{aligned} \quad (23)$$

$$\mu_4 = \frac{\sin 2\theta (m_2^2 - m_1^2) - 2\lambda_3 v_H v_S}{2v_H}, \quad (24)$$

$$\lambda_H = \frac{\cos 2\theta (m_1^2 - m_2^2) + m_1^2 + m_2^2}{4v_H^2}. \quad (25)$$

The scalar potential in the broken phase can be written as

$$\begin{aligned} V(h_1, h_2) &= \frac{m^2}{2} h_1^2 + \frac{M^2}{2} h_2^2 + d_1 h_1^3 + d_2 h_1^2 h_2 + d_3 h_1 h_2^2 + d_4 h_2^3 + z_1 h_1^4 \\ &\quad + z_2 h_1^3 h_2 + z_3 h_1^2 h_2^2 + z_4 h_1 h_2^3 + z_5 h_2^4, \end{aligned} \quad (26)$$

where d_i, z_i $i = 1, \dots, 5$ are expressed in terms of UV model parameters. The explicit expressions for coefficients relevant for Higgs pair production can be found in Appendix A.

3.1.1 Constraints on the parameter space

The scalar singlet model has a relatively vast parameter space, which we restrict by using theoretical and experimental constraints.

Vacuum stability: We demand that the potential $V(H, \Phi)$ is bounded from below, and we additionally impose that the electroweak vacuum corresponds to a (local) minimum. For large field values the relevant terms are

$$V(H, \Phi) \simeq \lambda_H (H^\dagger H)^2 + \frac{\lambda_2}{4} \Phi^4 + \frac{\lambda_3}{2} (H^\dagger H) \Phi^2. \quad (27)$$

Introducing $x \equiv H^\dagger H \geq 0$ and $y \equiv \Phi^2 \geq 0$, one may rewrite

$$V \simeq \left(\sqrt{\lambda_H} x - \frac{\sqrt{\lambda_2}}{2} y \right)^2 + \left(\frac{\lambda_3}{2} + \sqrt{\lambda_H \lambda_2} \right) x y. \quad (28)$$

It follows that the potential is bounded from below if

$$\lambda_H(\mu) > 0, \quad \lambda_2(\mu) > 0, \quad (29)$$

and, in addition, for $\lambda_3(\mu) < 0$,

$$\lambda_3(\mu) > -2\sqrt{\lambda_H(\mu)\lambda_2(\mu)} \quad \iff \quad 4\lambda_H(\mu)\lambda_2(\mu) - \lambda_3(\mu)^2 > 0. \quad (30)$$

To ensure that the electroweak vacuum is a local minimum, we also require the scalar mass matrix (the Hessian of V evaluated at the vacuum configuration) to be positive definite. In particular, a necessary condition is that its determinant is positive:

$$\det M^2 > 0, \quad (31)$$

which in our parametrization leads to

$$(2\lambda_H v_H^2) \left(2\lambda_2 v_S^2 + \mu_3 v_S - \frac{v_H^2 \mu_4}{2v_S} \right) > (\lambda_3^2 v_H^2 v_S^2 + \mu_4^2 v_H^2 + 2\lambda_3 \mu_4 v_H^2 v_S). \quad (32)$$

Perturbativity: We require perturbativity of the couplings from the electroweak scale up to Planck scale employing one-loop RGEs. This entails a generic upper bound on $|\lambda_i(\Lambda)| \leq 4\pi$, such that strongly coupled regime is avoided.

For coefficients with mass dimension one we require that the one-loop corrections to the trilinear Higgs self coupling are smaller than their tree-level values in the $SU(2)$ limit [65]. This leads to:

$$\frac{|\mu_4|}{\max(|\mu_2|, |\mu_1|)} \leq 4\pi, \quad \wedge \quad \left| \frac{\mu_3}{\mu_2} \right| \leq 4\pi. \quad (33)$$

Bounds on the couplings of the model can be imposed by exploiting perturbative unitarity [66]. We compute the partial wave amplitudes $a_{i,j \rightarrow kl}^0$ for $J = 0$ for every possible $2 \rightarrow 2$ scattering amplitude with i, j, k, l either h or S . We check that the model does not violate $|\text{Re}(a_{ij \rightarrow kl}^0)| < 1/2$, for each eigenvalue of the scattering matrix. In the vicinity of the poles the scattering amplitudes diverge as an indication that higher order corrections are needed. Since we are neglecting the width effects in this tree level analysis, we follow [67] and apply a kinematic cut of

$$\left| 1 - \frac{s}{m^2} \right| > 0.25, \quad (34)$$

where s denotes the Mandelstam variable for $2 \rightarrow 2$ and m is the Higgs mass.

Electroweak precision tests: As reported in [68] the strongest bound on the mixing angle comes from measurements of the W boson mass, M_W . Using the results of Ref. [69] a bound of $|\sin(\theta)| < 0.155$ holds for physical scalar singlet masses $m_2 > 800$ GeV. This bound is not updated to incorporate the more recent results of the ATLAS and CMS collaborations [70, 71] which further shrink the uncertainty, but no official combination exists so far.

Higgs coupling modifiers: Recent measurements from the ATLAS and CMS collaboration have fixed possible deviations for Higgs coupling to massive gauge bosons and to fermions in the framework of κ formalism [3, 4]. At 2σ confidence we have $\sin \theta \leq 0.3741$. This bound results less strong than the one of the M_W measurement.

3.1.2 Effective Field Theory for the singlet model

First we will discuss the contributions of the singlet model to SMEFT operators that modify the couplings entering the Higgs pair production process. As can be inferred from Refs. [72–74], the singlet model generates at tree-level the effective operators $\mathcal{O}_{H\square}$ and \mathcal{O}_H . In addition, it generates a contribution to $|H|^4$ that shifts λ_H to

$$\lambda_H \rightarrow \lambda_H - \frac{\mu_4^2}{\mu_2^2}.$$

The other Wilson coefficients are:

$$\frac{C_{H\square}}{\Lambda^2} = -\frac{\mu_4^2}{2\mu_2^4}, \quad (35)$$

$$\frac{C_H}{\Lambda^2} = -\frac{\lambda_3\mu_4^2}{2\mu_2^4} + \frac{\mu_3\mu_4^3}{3\mu_2^6}. \quad (36)$$

On-shell matching to the HEFT basis has been performed through a diagrammatic approach. We obtain:

$$\begin{aligned} c_{hVV} &= \cos \theta, & c_{hhVV} &= \cos^2 \theta - 2 \frac{\sin \theta v d_2}{m_2^2}, & c_{hhh} &= \frac{2v}{m_1^2} d_1, \\ c_t &= \cos \theta, & c_{2t} &= -\frac{\sin \theta v d_2}{m_2^2}. \end{aligned} \quad (37)$$

For the case of the color neutral scalar we do not get any contributions to c_{ggh} and c_{gghh} . An explicit example where they arise will be discussed in section 3.3. One can now do the exercise to understand where the SMEFT and HEFT couplings agree. Using the results of Table 1 and the relations among the parameters in Eqs. (24) one finds, expanding in large m_2 with respect to the other massive parameters and assuming in addition that θ is small,

$$\frac{C_{H\square}}{\Lambda^2} \approx \frac{v_S \lambda_3}{v_H m_2^2} \theta - \frac{1}{2v_H^2} \theta^2 + \frac{2m_1^2 - 2v_S^2 \lambda_2 - 5v_H^2 \lambda_3^2}{2v_H^2 m_2^2} \theta^2, \quad (38)$$

$$\frac{C_H}{\Lambda^2} \approx \frac{\lambda_3}{2v_H^2} \theta^2 + \frac{v_H^2 \lambda_3^2 - m_1^2 \lambda_3}{m_2^2 v_H^2} \theta^2. \quad (39)$$

Expanding in small θ and omitting in Eq. (38) and (39) terms of $\mathcal{O}(1/m_2^4)$ and $\mathcal{O}(\theta^2/m_2^2)$ we find the results in Table 2. Neglecting the terms of higher orders in $1/m_2^2$ indeed SMEFT and HEFT agree under the assumption of small mixing angles and $v_S \rightarrow 0$ (i.e. assuming that $v_S v_H \ll m_2^2$).

HEFT matching is not unique [75]. For instance one can adopt a different parameterisation of the singlet Lagrangian introducing a tadpole term but no v_S . In this case the matching to SMEFT does not contain the extra terms $\propto v_S$ and there is full agreement at $\mathcal{O}(\theta^2)$ [76]. The parameters though get re-interpreted. The recent Ref. [77] points out that choosing a parameter set consisting of masses, mixing angle and vacuum expectation values, as we use here, leads to maximally precise matching results. Finally, we notice that in Refs. [75, 78] which consider matching of the singlet model to HEFT further hierarchies

	HEFT	SMEFT
c_{hVV}	$1 - \frac{1}{2}\theta^2$	$1 - \frac{1}{2}\theta^2 + \frac{v_S v_H \lambda_3}{m_2^2} \theta$
c_{hhVV}	$1 - 2\theta^2$	$1 - 2\theta^2 + \frac{4v_S v_H \lambda_3}{m_2^2} \theta$
c_{hhh}	$1 - \frac{3}{2}\theta^2 + \frac{\lambda_3 v_H^2}{m_1^2} \theta^2$	$1 - \frac{3}{2}\theta^2 + \frac{\lambda_3 v_H^2}{m_1^2} \theta^2 + \frac{3v_H v_S \lambda_3}{m_2^2} \theta$
c_t	$1 - \frac{1}{2}\theta^2$	$1 - \frac{1}{2}\theta^2 + \frac{v_S v_H \lambda_3}{m_2^2} \theta$
c_{2t}	$-\frac{1}{2}\theta^2$	$-\frac{1}{2}\theta^2 + \frac{v_S v_H \lambda_3}{m_2^2} \theta$

Table 2: Relevant couplings in di-Higgs production up to $\mathcal{O}(\theta^3, \frac{\theta^2}{m_2^2}, \frac{1}{m_{h_2}^4})$.

among the UV parameters of the singlet model are imposed, which we do not need to impose here, nor are they necessary from the point of view of our power counting. As has been shown in Ref. [79], when assuming parametric hierarchies among the model parameters, the matching procedure directly determines whether the resulting low-energy description follows SMEFT or HEFT power counting. In particular, we notice that in the singlet model there is still parameter space allowed in which the linearisation of the mixing angle relation is not necessarily accurate. We are illustrating this, by showing in the following a comparison of couplings in HEFT and SMEFT relevant for Higgs pair production.

The coupling modifiers c_{hVV} and c_{hhVV} are shown in Fig. 1, by scanning over the pa-

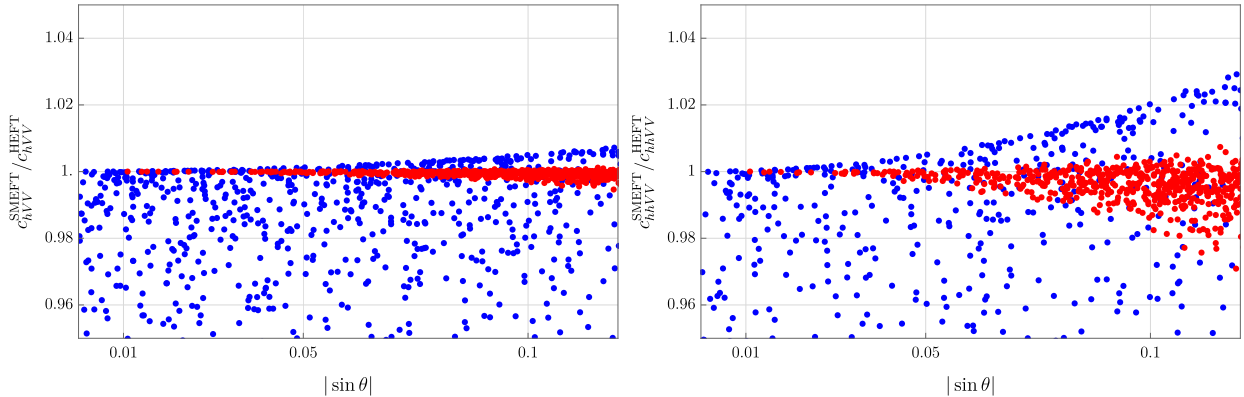


Figure 1: Ratio of the SMEFT and HEFT predictions for the coupling modifiers c_{hVV} and c_{hhVV} for a scan over the parameter space, using $\lambda_2 \in [0, 4\pi]$, $\lambda_3 \in [-4\pi, 4\pi]$, $|\sin \theta| < 0.15$, $v_S \in [0.01, 5v_H]$ and $M \in [2, 3]$ TeV (blue points). For the red points instead the range of v_S was constrained to lie within $v_S \in [0.01, 0.1v_H]$.

parameter space of the model imposing the conditions discussed in subsection 3.1.1. While the SMEFT and HEFT couplings agree well for small v_S the disagreement becomes larger for large v_S . The disagreement for small v_S points between SMEFT and HEFT is more pronounced for c_{hhVV} . This can be understood from the fact that, at $\mathcal{O}(\theta^3)$, terms proportional to $(v_H/v_S)\theta^3$ appear: for sufficiently small v_S , the enhancement by v_H/v_S can compensate the additional θ suppression, yielding a non-negligible contribution. While we do not show the plots for the other couplings, we note that we can see similar behaviour for c_t and c_{hhh} while the fact that we plot ratios, lead to a larger effect for c_{2t} where no SM coupling exists. We also comment on the fact that such a comparison on the level of couplings is not very physical. We could only do it as we were imposing the field redefinition in Eq. (7), otherwise in SMEFT at the considered order also new Lorentz structures would have contributed.

3.1.3 Results for gluon fusion into a Higgs pair

We compute inclusive cross section for Higgs pair production in gluon fusion using `hpair` [40, 80, 81] at LO in QCD. QCD corrections for gluon fusion Higgs pair production are large and their size depend on the EFT parameter point [82, 83]. But there is no public available code that allows to compute the NLO QCD corrections in full top mass dependence in the UV model. Adopting an infinite top mass limit the QCD corrections can be taken care of by a K factor that in this limit is basically independent on the specifics of the EFT parameter point [54, 81]. Such a K factor cancels in the ratios of cross sections we show in our figures. What regards the UV model, we also need the width of the heavy Higgs boson. We compute it using the Higgs width for a Higgs boson with mass m_2 using `hdecay` [84, 85] and add the partial width of the heavy Higgs boson decay to two light Higgs bosons given by

$$\Sigma_{h_2 \rightarrow h_1 h_1} = \frac{1}{16\pi m_2} d_2^2 \sqrt{1 - 4 \frac{m_1^2}{m_2^2}}. \quad (40)$$

We show our results as a function of f which measures the amount of symmetry breaking to the mass of the new scalar. Following [36] we define a f parameter such that $0 < f < 1$:

$$f = \frac{\lambda_3}{\lambda_3 + \frac{2\mu_2^2}{v_H^2}} = \frac{\lambda_3}{\lambda_3 + \lambda_{\text{ex}}}.$$

Moreover f is closely related to the expansion parameter appearing when one solves the equation of motion of the scalar singlet to obtain the effective operator expansion $r_{\text{exp}} = \frac{\lambda_3 v_H^2}{\mu_2^2}$. In fact these quantities may be related by:

$$f = \frac{\lambda_3}{\lambda_3 + \frac{\mu_2^2}{2v_H^2}} = \frac{2\lambda_3 v_H^2}{2\lambda_3 v_H^2 + \mu_2^2} = \frac{2r_{\text{exp}}}{1 + 2r_{\text{exp}}}.$$

When $f \rightarrow 1$ ($r_{\text{exp}} \rightarrow \infty$) the singlet acquires all its mass from electroweak symmetry breaking.

The results are collected in Fig. 2. The red and blue points originate from different parameter scans, imposing the bounds from subsection 3.1.1 and scanning as follows:

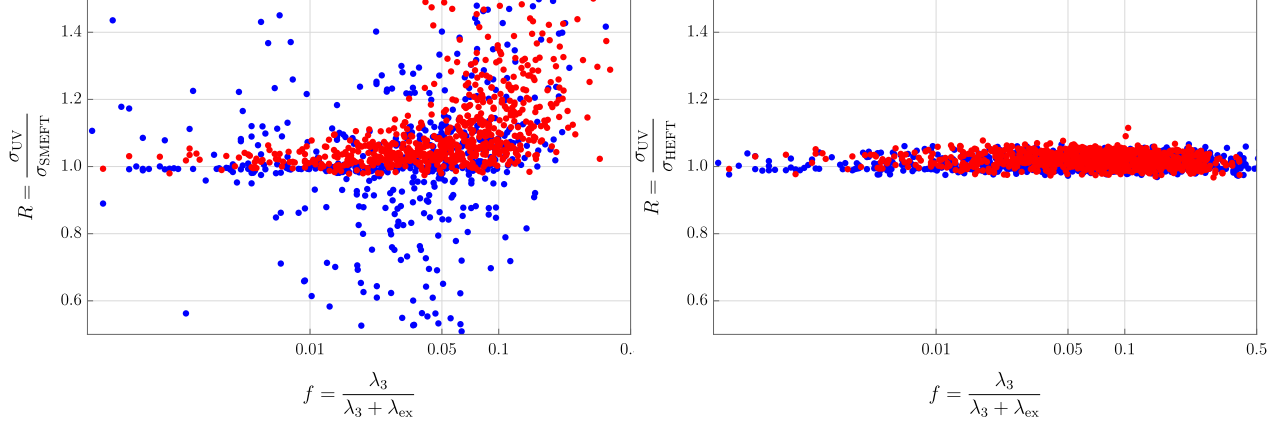


Figure 2: Cross section for Higgs production in gluon fusion using the scalar singlet model. On the right (left) panel we display ratio of σ_{UV} over the same quantity computed in HEFT (SMEFT) framework. Red (blue) points refer to scan 1 (scan 2) which allows for small values only (also order one values) of v_S/v_H .

$$\lambda_2 \in [0, 4\pi], \quad \lambda_3 \in [-4\pi, 4\pi], \quad |\sin \theta| \leq 0.15, \quad m_2 \in [800, 3000] \text{ GeV}, \quad (41)$$

and

- scan 1: $v_S \in [0.01, 0.1 v_H]$,
- scan 2: $v_S \in [0.01, 5 v_H]$.

While the values for the λ 's, the mixing angle and v_S are uniformly distributed over the range given in Eq. (41), the values of m_2 were chosen between normal distributions with mean 1800, 2200, 2600 GeV and standard deviation of 400 GeV. Since we truncate the cross section at $\mathcal{O}(1/\Lambda^2)$ it can happen that $\sigma_{\text{SMEFT}} < 0$. We interpret this as a breakdown of the SMEFT approximation [86]. In particular, we notice that this can happen in presence of high values of λ_3 i.e. high f values, implying that we are outside the convergence radius of SMEFT. The points with negative cross section are not shown in the plot as the y axis shows only positive values of $R = \sigma_{\text{UV}}/\sigma_{\text{SMEFT}}$. Figure 2 clearly shows that HEFT is the better EFT description for the considered model and parameter ranges. SMEFT can provide an accurate description if v_S and f are small.

3.1.4 Results for vector boson fusion into a Higgs pair

Vector boson fusion is the second biggest contribution for Higgs pair production at LHC. New physics effects dominantly affect the hard subprocess $VV \rightarrow hh$ where $V = W^\pm, Z$, while the forward tagging jets mostly provide a kinematic handle for event selection. We will hence concentrate on $VV \rightarrow hh$ and compare its unpolarized amplitude squared computed in the scalar singlet model with the same quantity computed in the EFT frameworks SMEFT and HEFT.² We computed the amplitudes at different centre of mass (c.o.m.) energies \sqrt{s}

²For a similar study in the context of the triplet extension of the SM, see Ref. [87].

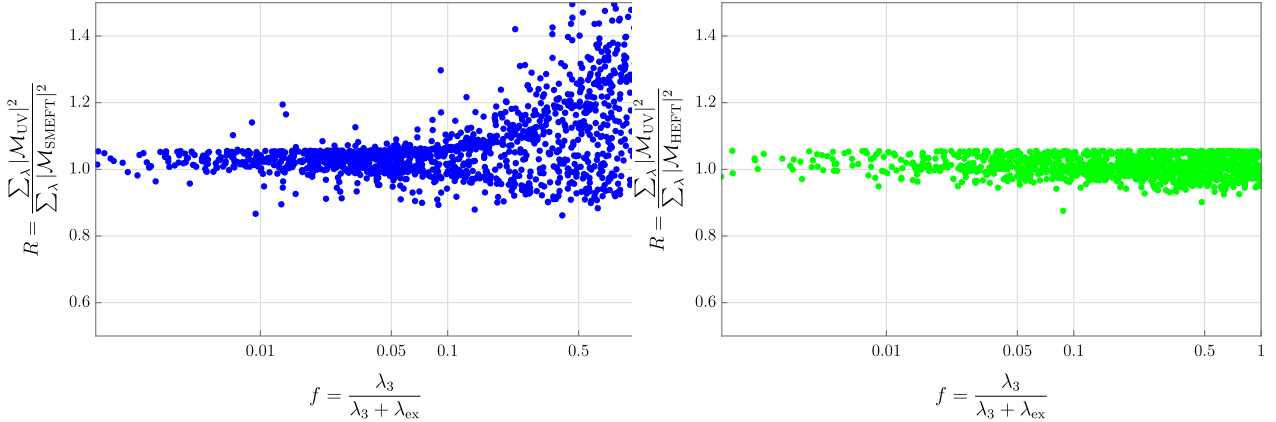


Figure 3: Unpolarized amplitudes squared for Higgs pair production in vector boson fusion for the scalar singlet model. On the right (left) panel we display the ratio of the unpolarized amplitude squared in the UV model over the same quantity computed in HEFT (SMEFT) framework .

at fixed value of the scattering angle. Since no significant qualitative difference has shown up at different values of \sqrt{s} we refrain to compute the full cross sections. We also note that the QCD corrected cross sections are basically insensitive to the specifics of the EFT parameter point [88, 89].

Our results are summarized in Fig. 3. The points displayed in the figure result from a scan in the parameter space similar to the one in Eq. (41) but using

$$v_S \in [0.2v_H, 2v_H]. \quad (42)$$

Scans which allow higher values of v_S follow a very similar behaviour as the one shown. In Fig. 3 we have fixed the scattering angle to its maximal value $\alpha_{\max} = \frac{\pi}{2}$ and $\sqrt{s} = 1$ TeV. The SMEFT amplitudes $\mathcal{M}_{\text{SMEFT}} = \mathcal{M}_{\text{SM}} + \frac{c}{\Lambda^2} \mathcal{M}^{(6)}$ were computed under linearised SMEFT approximation $|\mathcal{M}_{\text{SMEFT}}|^2 = |\mathcal{M}_{\text{SM}}|^2 + 2\frac{c}{\Lambda^2} \text{Re}(\mathcal{M}_{\text{SM}} \mathcal{M}^{(6)}) + \mathcal{O}(1/\Lambda^4)$ i.e. neglecting dimension-8 contributions stemming from the matrix element squared. We checked though explicitly that basically no difference emerges when including those terms of $\mathcal{O}(1/\Lambda^4)$ stemming from $\text{Re}(\mathcal{M}_{\text{SM}} \mathcal{M}^{(6)})$.

From Fig. 3 we interfere that while for $f < 0.1$ SMEFT and HEFT do nearly equally well, for larger values of f HEFT seems to describe the full UV model better. While Fig. 3 is for fixed \sqrt{s} and scattering angle, one can observe that for higher (lower) values of \sqrt{s} SMEFT describes the UV model well up to higher (lower) values of f with respect to $f = 0.1$, HEFT does not show significant deviation.

3.2 Two Higgs Doublet Model

The two Higgs doublet model (2HDM) [90] is constructed by adding a second $SU(2)$ doublet Φ_2 to the spectrum of the SM. In the following we will slightly change notation and nominate both the Higgs doublets by Φ_i with $i = 1, 2$. We assume CP-conservation and impose a \mathbb{Z}_2

symmetry on the potential that acts as $\Phi_1 \rightarrow \Phi_1$ and $\Phi_2 \rightarrow -\Phi_2$. This symmetry assignment avoids flavour-changing neutral currents and is softly-broken by an off-diagonal mass term m_{12} . The spectrum of the 2HDM contains two CP-even neutral Higgs bosons h and H , a CP-odd Higgs boson A and two charged Higgs bosons H^\pm . The potential can then be written as

$$\begin{aligned} V(\Phi_1, \Phi_2) = & m_{11}^2(\Phi_1^\dagger \Phi_1) + m_{22}^2(\Phi_2^\dagger \Phi_2) - m_{12}^2 [\Phi_1^\dagger \Phi_2 + \text{h.c.}] + \frac{\lambda_1}{2}(\Phi_1^\dagger \Phi_1)^2 + \frac{\lambda_2}{2}(\Phi_2^\dagger \Phi_2)^2 \\ & + \lambda_3(\Phi_1^\dagger \Phi_1)(\Phi_2^\dagger \Phi_2) + \lambda_4(\Phi_1^\dagger \Phi_2)(\Phi_2^\dagger \Phi_1) + \frac{\lambda_5}{2} [(\Phi_1^\dagger \Phi_2)^2 + \text{h.c.}] . \end{aligned} \quad (43)$$

Each of the doublets can acquire a vacuum expectation value $\langle \Phi_1 \rangle = v_1/\sqrt{2}$ and $\langle \Phi_2 \rangle = v_2/\sqrt{2}$ with $v^2 = v_1^2 + v_2^2 = (246 \text{ GeV})^2$. The angle β with $\tan \beta = v_2/v_1$ diagonalises the charged pseudoscalar Higgs sector. It is useful to rotate the original doublets into the *Higgs basis*

$$\begin{pmatrix} H_1 \\ H_2 \end{pmatrix} = \begin{pmatrix} c_\beta & s_\beta \\ -s_\beta & c_\beta \end{pmatrix} \begin{pmatrix} \Phi_1 \\ \Phi_2 \end{pmatrix}, \quad (44)$$

with $c_\beta = \cos \beta$ and $s_\beta = \sin \beta$, in which only one of the doublets acquires a vacuum expectation value, namely $\langle H_1 \rangle = v/\sqrt{2}$ and $\langle H_2 \rangle = 0$. The potential in the Higgs basis reads

$$\begin{aligned} V(H_1, H_2) = & M_{11}^2(H_1^\dagger H_1) + M_{22}^2(H_2^\dagger H_2) - M_{12}^2 [H_1^\dagger H_2 + \text{h.c.}] \\ & + \frac{\Lambda_1}{2}(H_1^\dagger H_1)^2 + \frac{\Lambda_2}{2}(H_2^\dagger H_2)^2 + \Lambda_3(H_1^\dagger H_1)(H_2^\dagger H_2) + \Lambda_4(H_1^\dagger H_2)(H_2^\dagger H_1) \\ & + \left[\frac{\Lambda_5}{2}(H_1^\dagger H_2)^2 + \Lambda_6(H_1^\dagger H_1)(H_1^\dagger H_2) + \Lambda_7(H_1^\dagger H_2)(H_2^\dagger H_2) + \text{h.c.} \right] . \end{aligned} \quad (45)$$

The relations between the parameters of the Higgs basis potential and the potential in Eq. (43) can be found in full generality in Appendix A of Ref. [91]. In order to obtain the physical Higgs bosons, a rotation

$$\begin{pmatrix} H \\ h \end{pmatrix} = \begin{pmatrix} c_{\beta-\alpha} & s_{\beta-\alpha} \\ -s_{\beta-\alpha} & c_{\beta-\alpha} \end{pmatrix} \begin{pmatrix} H_1^0 \\ H_2^0 \end{pmatrix}, \quad (46)$$

where H_i^0 denotes the neutral CP-even component of H_i , is performed. Finally, we note that all the physical heavy Higgs boson masses m_{H^\pm} , m_A and m_H obtain a component of an explicit mass term and a mass component from electroweak symmetry breaking. For instance we can write

$$m_H^2 = M^2 + \tilde{\Lambda} v^2 \quad (47)$$

where $\tilde{\Lambda}$ is a combination of the λ_i (see e.g. Ref. [92]) and

$$M^2 = \frac{m_{12}^2}{\sin \beta \cos \beta}. \quad (48)$$

We use as input parameters

$$m_h, \quad m_H, \quad m_A, \quad m_{H^\pm}, \quad t_\beta = \tan \beta, \quad c_{\beta-\alpha}, \quad M^2. \quad (49)$$

3.2.1 Matching to HEFT and SMEFT

We match the 2HDM to HEFT and SMEFT. The matching to SMEFT is well known and has been computed up to dimension 8 in [93] and at one-loop order in [94]³. For the couplings relevant for Higgs pair production in gluon fusion, one finds, matching at tree level [94],

$$\frac{C_{tH}}{\Lambda^2} = \frac{y_u \Lambda_6}{M^2 \tan \beta} = -\frac{\sqrt{2}}{v^3} \frac{c_{\beta-\alpha}}{t_\beta} m_t - \frac{1}{\sqrt{2} v^3} \left(c_{\beta-\alpha}^2 + \frac{c_{\beta-\alpha}(4\Delta m_H^2 - 6m_h^2)}{t_\beta \Lambda^2} \right) m_t, \quad (50)$$

$$\frac{C_H}{\Lambda^2} = \frac{\Lambda^2}{v^4} c_{\beta-\alpha}^2 + \frac{4}{v^4} c_{\beta-\alpha}^2 (\Delta m_H^2 - m_h^2). \quad (51)$$

Λ takes the role of the heavy masses that are assumed to be degenerate and

$$\Lambda^2 = M^2 - \frac{1}{2} (s_{\beta-\alpha}^2 m_h^2 + c_{\beta-\alpha}^2 m_H^2) - c_{\beta-\alpha} s_{\beta-\alpha} \tan(2\beta) (m_h^2 - m_H^2), \quad (52)$$

whereas $\Delta m_H^2 = m_H^2 - \Lambda^2$. Instead for HEFT we find

$$c_t = s_{\beta-\alpha} + \frac{c_{\beta-\alpha}}{t_\beta}, \quad (53)$$

$$c_{hhh} = \frac{2v}{m_1^2} d_1^{\text{2HDM}}, \quad (54)$$

$$c_{2t} = -\frac{(c_{\beta-\alpha} - \frac{s_{\beta-\alpha}}{t_\beta}) v d_2^{\text{2HDM}}}{m_H^2}, \quad (55)$$

with d_i^{2HDM} given in Appendix A. In analogy to our considerations for the singlet model, we want to understand in which limit the couplings correspond to each other in SMEFT and HEFT. We expand in small mixing angle, noting that the SMEFT limit of large Lagrangian mass corresponds to small mixing between light and heavy Higgs bosons, $c_{\beta-\alpha} \ll 1$. The results of this expansion can be found in Table 3.

We note that even in the limit of small $c_{\beta-\alpha}$ the functional forms of c_{hhh} , c_t , and c_{2t} in HEFT and SMEFT is different. In the limit, $v \rightarrow 0$ and using Eq. (47) we see though that the SMEFT and HEFT coupling agree, again clearly showing that SMEFT is an expansion in a large Lagrangian parameter, here M^2 , while HEFT expands in large physical mass. In the following, we will compare HEFT and SMEFT predictions in gluon fusion, while we expect in vector boson fusion less interesting effects due to the suppression of the effects in Higgs vector-boson couplings, starting only at order $c_{\beta-\alpha}^2$.

3.2.2 Theoretical and experimental constraints on the model

In order to take into account constraints on the parameter space we follow the discussion of Ref. [96].

³See also [95] for the choice of an especially convenient choice of basis.

	HEFT	SMEFT
c_{hhh}	$1 - 2 \frac{M^2}{m_h^2} c_{\beta-\alpha}^2$	$1 - 2 \frac{4m_H^2 - 3M^2}{m_h^2} c_{\beta-\alpha}^2$
c_t	$1 + \frac{c_{\beta-\alpha}}{t_\beta}$	$1 + \frac{c_{\beta-\alpha}}{t_\beta} + 2 \frac{m_H^2 - M^2}{t_\beta M^2}$
c_{2t}	$4 \frac{M^2}{m_H^2} \frac{c_{\beta-\alpha}}{t_\beta} - \frac{c_{\beta-\alpha}}{t_\beta}$	$3 \frac{c_{\beta-\alpha}}{t_\beta} + 6 \frac{m_H^2 - M^2}{t_\beta M^2}$

Table 3: Relevant couplings in di-Higgs production up to $\mathcal{O}(c_{\beta-\alpha})$ for the 2HDM. c_{hVV} becomes equal to one at the considered order. The trilinear Higgs self-coupling has been expanded an order higher in $c_{\beta-\alpha}$, see text.

Vacuum stability: We require boundedness from below, leading to the criteria

$$\lambda_1 \geq 0, \quad (56)$$

$$\lambda_2 \geq 0, \quad (57)$$

$$\lambda_3 + \sqrt{\lambda_1 \lambda_2} \geq 0, \quad (58)$$

$$\lambda_3 + \lambda_4 - |\lambda_5| + \sqrt{\lambda_1 \lambda_2} \geq 0, \quad (59)$$

implemented as a required condition when scanning over the parameter space.

Perturbativity: Requiring that the eigenvalues of the lowest partial wave matrix remain below 16π puts bounds on the values of the scalar potential λ_i . The conditions can be found in [96] and we implement them as a required condition to keep a point in a scan over the parameter space.

Electroweak precision tests: Assuming that the heavy Higgs boson masses are degenerate either $m_A \sim m_{H^\pm}$ or $m_H \sim m_{H^\pm}$ avoids constraints from electroweak precision tests. Since we do not need to specify the masses m_A or m_{H^\pm} in our analysis we can trivially satisfy the constraints imposed by electroweak precision tests.

Flavour physics: Flavour physics, in particular the decays $B_s \rightarrow X_s \gamma$ and $B_s \rightarrow \mu^+ \mu^-$ can impose important bounds on the value of $\tan \beta$ for light and moderate values of m_{H^\pm} . Those limits depend on the type of 2HDM considered. Since we consider the EFT limit, assuming that the heavy Higgs boson masses are larger than 1 TeV, we can evade them both in the type I and type II 2HDM by imposing in our scan that $\tan \beta > 0.9$.

Higgs coupling measurements: In order to assure that the SM-like Higgs boson fulfills constraints from experimental Higgs coupling measurements, we use the results of the ATLAS SMEFT scan in Ref. [97]. This means that we match to the SMEFT at

tree level and keep a point in parameter space if the $\chi^2 < \chi_{min}^2 + 5.99$. The χ_{min} is determined within the physical allowed range for $\tan \beta$ (see below).

We generate points in parameter space that fulfill these conditions, scanning over the parameter space with

$$c_{\beta-\alpha} \in [-0.2, 0.2], \quad \tan \beta \in [0.9, 50], \text{GeV}^2, \quad m_H \in [1000, 3000] \text{GeV}. \quad (60)$$

We restrict the value of $c_{\beta-\alpha}$ to the shown range to improve the effectiveness of the scan taking into account already typical constraints stemming from Higgs coupling measurements. We generate M^2 in a Gaussian distribution around $m_H^2 \cos^2 \alpha / \sin^2 \beta$ [96] to obtain more efficiently points that fulfill the requirement of stability and perturbativity constraints. Those depend also on the masses m_A and m_{H^\pm} that we in principle do not need to specify for our analysis. We address this by setting $m_A = m_{H^\pm}$ as required by electroweak precision tests and scan in steps the remaining parameter to check whether perturbativity and partial wave unitarity can be fulfilled for any value of $m_{H^\pm}^2 \in [10^6, 10^9] \text{GeV}^2$. We consider two realisations of the 2HDM, the type I and the type II model. In our parameter scan, the only difference in the model arises from the Higgs coupling measurements. While in the type I model the Yukawa type operator C_{fH} is the same for up-type, down-type and leptons (the only difference in Eq. (50) is that the top mass is to be replaced by the respective fermion mass), in the type II model the Yukawa-type operator of down-type fermions and leptons is given by

$$\frac{C_{fH}}{\Lambda^2} = \frac{\sqrt{2}}{v^3} c_{\beta-\alpha} t_\beta m_f - \frac{1}{\sqrt{2}v^3} \left(c_{\beta-\alpha}^2 - \frac{t_\beta c_{\beta-\alpha} (4\Delta m_H^2 - 6m_h^2)}{\Lambda^2} \right) m_f, \quad (61)$$

with $f = b, s, d, \tau, \mu, e$. As a consequence a much smaller parameter space survives the bounds on Higgs coupling measurements in the type II model with respect to the type I model [97]. In particular one is constrained to smaller values of $c_{\beta-\alpha}$ and t_β .

3.2.3 Results for gluon fusion into a Higgs boson pair

In Fig. 4 we present the result for the type I and type II model. The points are compatible with the constraints one the parameter space imposed in subsection 3.2.2. In order to compute the heavy Higgs width, needed for the UV model predictions, we have used `hdecay` [84, 85]. In the cross section computation, we have only considered the top quark loops, which is motivated by the fact that in the SM the bottom loops are strongly suppressed [27]. They could play a larger role in the type II model at large t_β . Since points with a large enhancements in the bottom couplings are though excluded by Higgs coupling measurements, this is a safe approximation.

As can be inferred from Fig. 4, the type II model allows for larger deviations from the alignment limit and as such we also find larger differences between the SMEFT and HEFT descriptions. The HEFT describes the UV model very well for positive values of $c_{\beta-\alpha}$, i.e. the ratio shown in the plot by the black points is very close to 1. In SMEFT, the ratio between EFT and UV result as shown by the orange points which deviate more and more from 1 with increasing value of $c_{\beta-\alpha}$. The effect is much smaller in the type II model as $c_{\beta-\alpha}$ is much more constrained. For our points with negative signs of $c_{\beta-\alpha}$ also the sign of the coupling of the heavy Higgs boson to top quarks is flipped, whereas the heavy to light

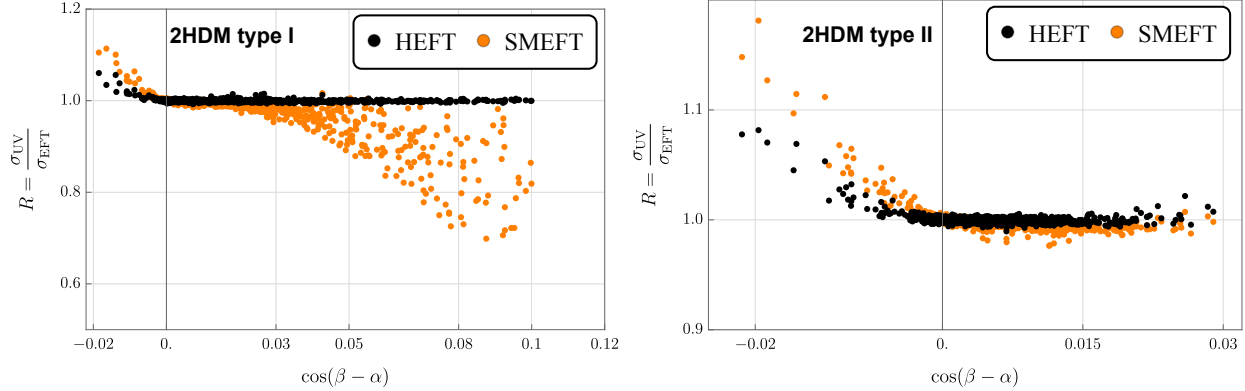


Figure 4: Ratio of the full model cross section over the EFT cross section, for the 2HDM of type I (left) and type II (right). The black points show the case of matching to the HEFT and the orange points show the case of matching to the SMEFT.

Higgs self coupling remains positive hence changing the interference with the continuum in $gg \rightarrow hh$. Having a delicate interference structure, amplifies the mismatch of truncated EFT descriptions for $c_{\beta-\alpha} < 0$.

For the SMEFT, we have considered only orders of to $1/\Lambda^2$ in the cross section. In EFT analysis, sometimes SMEFT is instead truncated at order $1/\Lambda^2$ at the level of the matrix element, allowing hence terms of order $1/\Lambda^4$ in the cross section. In Fig. 5 we show the same as the left plot of Fig. 4 for the type I model but truncated at the level of the matrix element. We see that indeed this choice worsens the agreement between the EFT and UV descriptions of the model.

A comment on the choice of $c_{\beta-\alpha}$ as x axis is in order. Similar to the singlet case, one could have defined a parameter f that measures how much mass comes from electroweak symmetry breaking and how much from an explicit mass parameter in the Lagrangian. In that respect, for instance an $f = (m_H^2 - M^2)/M^2$ could have been defined. We note however given our choice of m_H to be above 1 TeV to remain in an EFT regime and imposing vacuum stability and perturbativity automatically selects only small values of f making $c_{\beta-\alpha}$ the decisive parameter.⁴

Finally, we note that we have performed the matching only at tree level. It is well known that loop corrections to the trilinear Higgs self-couplings can be largely enhanced with respect to the tree-level in the 2HDM even in the alignment limit $c_{\beta-\alpha} \rightarrow 0$ in the presence of large scalar potential couplings, see e.g. [98–103]. In this respect, it might be interesting to see how well HEFT describes the full model including also higher orders both in the matching and the full model. Since even the two-loop corrections are large, this is clearly beyond the scope of this work.

⁴This is also in line with the findings of [38] which shows that Loryons with values of $f > 0.5$ have masses up to 700 GeV. We note though that our model is a bit different from the one in the study of [38] as they have no soft breaking of the \mathbb{Z}_2 symmetry.

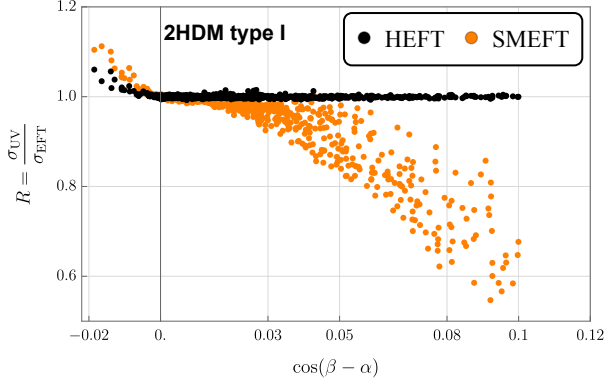


Figure 5: Ratio of the full model cross section over the EFT cross section, for the 2HDM of type I truncating the SMEFT at $\mathcal{O}(1/\Lambda^2)$ at the matrix element level, while keeping quadratic terms in the cross section.

3.3 Colored scalars

In this section we study a colored scalar ω_1 whose charges under SM group are $(3, 1)_{-1/3}$, where the numbers indicate the $(SU(3), SU(2)_L)_Y$ representations or charges. The SM Lagrangian is extended by

$$\mathcal{L} \supset D_\mu \omega_1^\dagger D^\mu \omega_1 - M_{\text{ex}}^2 \omega_1^\dagger \omega_1 - \frac{c_{\lambda\phi}}{2} \omega_1^\dagger \omega_1 H^\dagger H. \quad (62)$$

In Eq. (62), the first term contains the covariant derivative which couples ω_1 to the gauge sector, the second piece is the explicit mass term and the last one represents a Higgs-portal interaction which provides another contribution to ω_1 mass in the broken phase. The Feynman rules generated by Eq. (62) relevant for our computation are presented in Appendix C.

3.3.1 Effective field theory for the colored scalar

Here we compute the contributions to the effective operators affecting gluon fusion Higgs production. What regards the matching of the color scalar model, we stay strictly at the one-loop order, so keep the one-loop matching contributions to \mathcal{O}_{HG} as the operator enters at tree level, but neglect the effect of one-loop matching to C_H as this would be effectively be a two-loop contribution to the gluon fusion process. The beyond-the SM scattering amplitude in SMEFT up to dimension 6, cross-checked with **SMEFTsim** [104], is

$$\begin{aligned} \mathcal{M}_{\text{SMEFT}}(gg \rightarrow hh) = & \frac{24 C_{HG} \lambda_H v_H^2 \delta^{ab} \varepsilon^\mu(p_1) \varepsilon^\nu(p_2) (p_2^\mu p_1^\nu - g^{\mu\nu}(p_1 \cdot p_2))}{\Lambda^2 (s - m_H^2)} \\ & + \frac{4 C_{HG} \delta^{ab} \varepsilon^\mu(p_1) \varepsilon^\nu(p_2) (p_2^\mu p_1^\nu - g^{\mu\nu}(p_1 \cdot p_2))}{\Lambda^2} + \mathcal{O}\left(\frac{v_H^4}{\Lambda^4}\right), \end{aligned} \quad (63)$$

where the ingoing gluons have color indices a, b , momenta p_1^μ and p_2^ν and are assumed to be on-shell. We denote the metric tensor with $(1, -1, -1, -1)$ signature by $g_{\mu\nu}$. The Wilson

coefficient, computed with **Matchete** [105], is

$$\frac{C_{HG}}{\Lambda^2} = \frac{1}{4\pi} \frac{\alpha_s(\mu) c_{\lambda\phi}}{48M_{\text{ex}}^2}. \quad (64)$$

In the broken phase this terms generates two effective couplings of the Higgs boson with gluons. We recall our normalization for later convenience:

$$\Delta\mathcal{L}_{\text{SMEFT}}^{b.p.} \supset \frac{\alpha_s}{8\pi} \left(c_{ggh}^{\text{SMEFT}} \frac{h}{v} + c_{gghh}^{\text{SMEFT}} \frac{h^2}{v^2} \right) G_{\mu\nu}^a G^{a,\mu\nu}, \quad c_{ggh}^{\text{SMEFT}} = \frac{c_{\lambda\phi} v_H^2}{24M_{\text{ex}}^2}, \quad c_{gghh}^{\text{SMEFT}} = \frac{c_{\lambda\phi} v_H^2}{48M_{\text{ex}}^2}. \quad (65)$$

Analogously to the scalar singlet case, on-shell matching to the HEFT basis has been performed through a diagrammatic approach at the one-loop level. Taking $M_{\text{Loryon}}^2 = M_{\text{ex}}^2 + \frac{c_{\lambda\phi} v_H^2}{4}$ or equivalently $M_{\text{Loryon}}^2 = M_{\text{ex}}^2 + \Delta M_{\text{Loryon}}^2$ the effective couplings read:

$$c_{ggh} = \frac{c_{\lambda\phi} v_H^2}{24M_{\text{Loryon}}^2} = \frac{\Delta M_{\text{Loryon}}^2}{6M_{\text{Loryon}}^2}, \quad (66)$$

$$c_{gghh} = \frac{c_{\lambda\phi} v_H^2}{48M_{\text{Loryon}}^2} - \frac{(c_{\lambda\phi} v_H^2)^2}{96M_{\text{Loryon}}^4} = \frac{\Delta M_{\text{Loryon}}^2}{12M_{\text{Loryon}}^2} - \frac{\Delta M_{\text{Loryon}}^4}{6M_{\text{Loryon}}^4}. \quad (67)$$

Similarly to the other cases discussed before, the SMEFT predicts a linear relation among the effective couplings being $c_{gghh}^{\text{SMEFT}} = 1/2 c_{ggh}^{\text{SMEFT}}$. The relation is broken in HEFT due to the contribution of the last term in Eq. (67). In the limit $M_{\text{ex}}^2 \gg c_{\lambda\phi} v_H^2$, we see though that $c_{ggh} = c_{ggh}^{\text{SMEFT}}$ and $c_{gghh} = c_{gghh}^{\text{SMEFT}}$, so the SMEFT relation is re-established. Indeed, this is in analogy to the case of a heavy quark loop in gluon fusion: as stated in [106] models where the quark gets its whole mass from electroweak symmetry breaking match to an operator

$$\log \left(\frac{H^\dagger H}{v^2} \right) G_{\mu\nu}^a G^{a,\mu\nu} \quad (68)$$

while quarks that get mass from an explicit mass term match to \mathcal{O}_{HG} . General models give something in between.

3.3.2 Results for gluon fusion into a Higgs pair

In Fig. 6 we present the results for this model as a function of $c_{\lambda\phi}$ for a mass of $m_{\omega_1} = 1$ TeV. We have explicitly checked that when computing all the matching coefficients at one-loop level in the model, Higgs measurements do not lead to any relevant bound on $c_{\lambda\phi}$, on which we hence impose by perturbative unitarity $|c_{\lambda\phi}| < 4\pi$. As can be inferred from Fig. 6, the color scalar model is slightly better described by HEFT than by SMEFT. The cross section though changes only little with respect to the SM value even for large $c_{\lambda\phi}$, much below the theoretical uncertainty for the gluon fusion cross section [107].

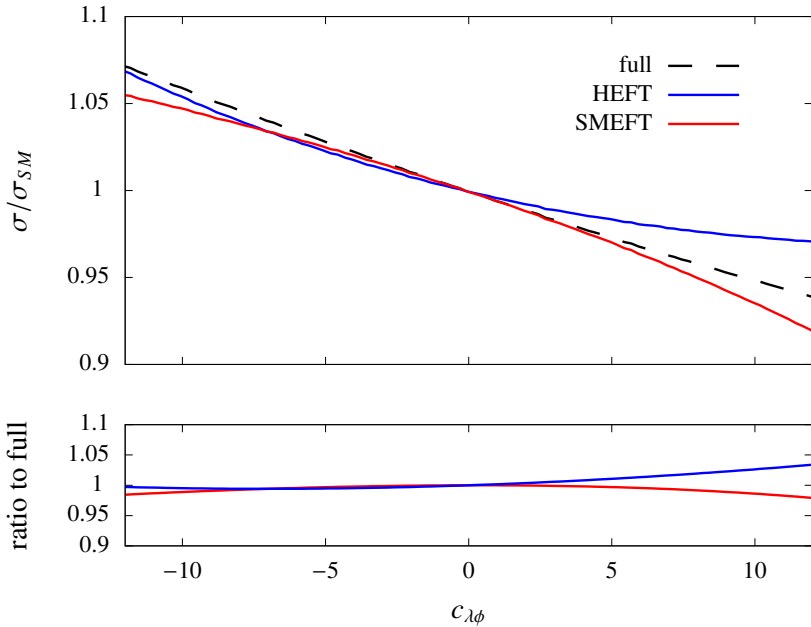


Figure 6: *Upper pannel:* Cross section divided by the SM value for the UV model of a colored scalar (black dashed), HEFT (blue) and SMEFT (red) setting $M_{\text{Loryon}} = 1 \text{ TeV}$. *Lower pannel:* Ratio of SMEFT (red) and HEFT (blue) cross section with respect to the cross section in the UV model.

4 Conclusion

In this work, we investigate whether new-physics effects in Higgs pair production require a HEFT description, or whether they can be adequately captured within SMEFT. Since current experimental searches are performed within the framework of dimension-6 SMEFT and the LO HEFT Lagrangian, we restrict our analysis accordingly.

To address this question, we studied three models that can act as so-called Loryons – particles that acquire more than half their mass from electroweak symmetry breaking and are thus better suited to HEFT than SMEFT descriptions. These include the scalar singlet extension, the 2HDM, and an extension with a colored scalar. At tree level, the singlet model generates contributions to $C_{H\square}$ and C_H , leading to a general rescaling of Higgs couplings and modifications to the trilinear Higgs self-coupling. The 2HDM additionally generates contributions to C_{tH} , modifying the Higgs couplings to top quarks while keeping the Higgs to vector boson couplings unaffected, and the colored scalar model generates contributions to C_{HG} at one-loop order.

We explicitly demonstrated the conditions under which the relevant HEFT and SMEFT couplings agree. This connection relates to the fact that HEFT assumes large physical masses, whereas SMEFT matching is performed in the unbroken phase as an EFT expansion in a large Lagrangian mass parameter.

Our results explicitly show that for both the singlet and 2HDM, there exists viable

parameter space where HEFT provides a demonstrably better description of the UV model than SMEFT. For the colored scalar, however, since we considered loop-induced couplings, the difference in the cross section relative to the SM was sufficiently small to fall below measurement uncertainty.

Finally, we note that our study was restricted to the dominant EFT contributions – tree-level matching for the singlet and 2HDM, and one-loop matching for the colored scalar. Furthermore, we considered only leading-order HEFT and dimension-6 SMEFT. Future extensions of this study could incorporate loop effects and higher orders in the EFT expansion.

Acknowledgements

RG thanks Ilaria Brivio and Konstantin Schmid for endless HEFT discussions. The work of RG is supported by a STARS@UniPD grant under the acronym “HiggsPairs” and in part by the Italian MUR Departments of Excellence grant 2023-2027 ”Quantum Frontiers”. The authors acknowledge support from the COMETA COST Action CA22130.

A Definition of HEFT coefficients

In this appendix we collect the relevant quantities for the matching to HEFT.

A.1 Scalar singlet model

For the scalar singlet model discussed in section 3.1 we give the analytic expression for the light Higgs boson h self couplings and the couplings of a heavy Higgs boson to two light Higgs bosons in terms of the model parameters:

$$d_1 = v_H \lambda_H \cos^3 \theta - \frac{1}{2} \lambda_3 v_S \cos^2 \theta \sin \theta - \frac{\mu_4}{2} \cos^2 \theta \sin \theta + \frac{1}{2} \lambda_3 v_H \cos \theta \sin^2 \theta - \lambda_2 v_S \sin^3 \theta - \frac{\mu_3}{3} \sin^3 \theta, \quad (69)$$

$$d_2 = \frac{1}{2} \lambda_3 v_S \cos^3 \theta + \frac{1}{2} \mu_4 \cos^3 \theta + 3 \lambda_H v_H \cos^2 \theta \sin \theta - \lambda_3 v_H \cos^2 \theta \sin \theta + 3 v_S \lambda_2 \cos \theta \sin^2 \theta + \mu_3 \cos \theta \sin^2 \theta - \mu_4 \cos \theta \sin^2 \theta - \lambda_3 v_S \cos \theta \sin^2 \theta + \frac{1}{2} \lambda_3 v_H \sin^3 \theta. \quad (70)$$

A.2 Two Higgs doublet model

For the 2HDM, we take the Higgs self-couplings necessary for the HEFT matching in Eqs. (54) and (55) from Ref. [108]:

$$d_1^{2\text{HDM}} = \frac{3}{2v^2} [s_{\beta-\alpha}^3 m_h^2 + s_{\beta-\alpha} c_{\beta-\alpha}^2 (3m_h^2 - 2M^2) + 2c_{\beta-\alpha}^3 \cot 2\beta (m_h^2 - M^2)], \quad (71)$$

$$d_2^{2\text{HDM}} = \frac{-c_{\beta-\alpha}}{v^2} [s_{\beta-\alpha}^2 (2m_h^2 + m_H^2 - 4M^2) + 2s_{\beta-\alpha} c_{\beta-\alpha} \cot 2\beta (2m_h^2 + m_H^2 - 3M^2) - c_{\beta-\alpha}^2 (2m_h^2 + m_H^2 - 2M^2)]. \quad (72)$$

B Singlet Model: mixing angle dependence

Here we show Fig. 7 already presented as Fig. 2 but as function of the mixing angle $\sin \theta$.

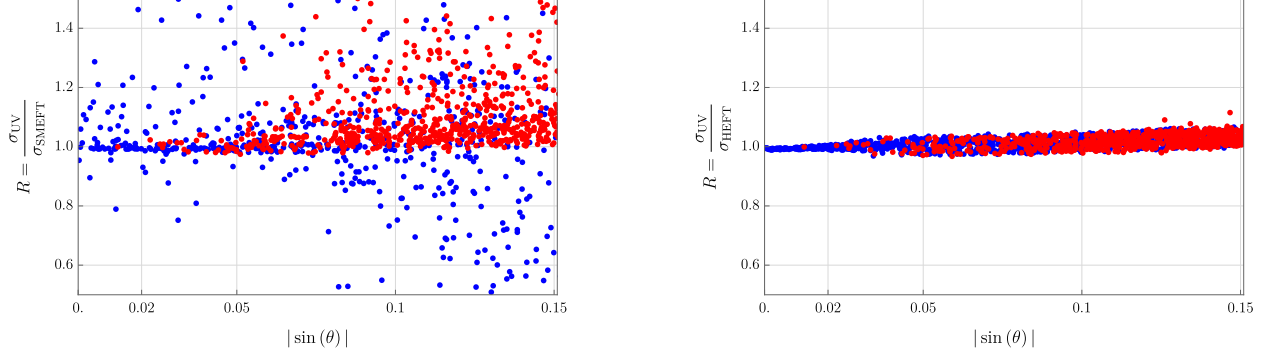
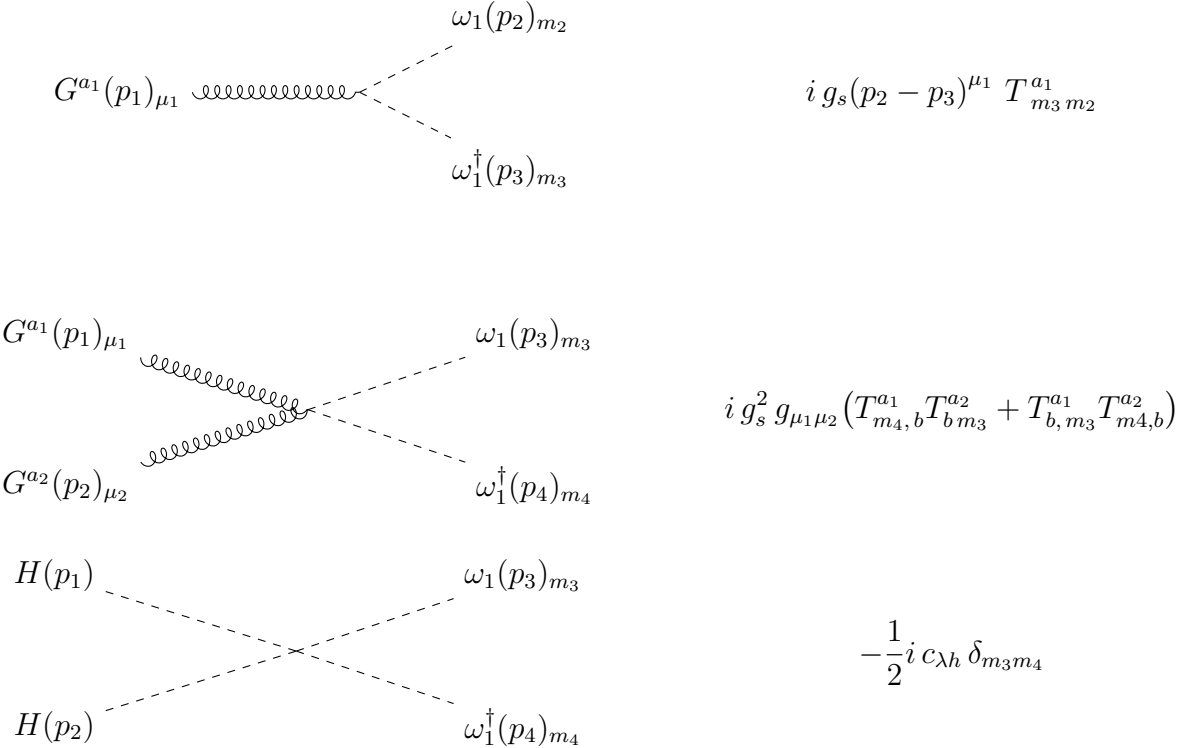


Figure 7: Same as Fig. 2, but shown in terms of $|\sin \theta|$.

C Feynman Rules for the Colored Scalar Model

Here we present the Feynman rules needed for the computation of the cross sections for the colored scalar model. They were obtained with `FeynRules` [109]. T^a are the colour matrices with a generic matrix element written as $T_{m_i m_j}^a$.



$$\begin{aligned}
& \omega_1(p_2)_{m_2} \\
H(p_1) \text{-----} & \leftarrow \text{dashed line} \\
& \omega_1^\dagger(p_3)_{m_3}
\end{aligned}$$

$$-\frac{1}{2}i v_H c_{\lambda h} \delta_{m_2 m_3}$$

References

- [1] **ATLAS** Collaboration, G. Aad *et al.*, “Observation of a new particle in the search for the Standard Model Higgs boson with the ATLAS detector at the LHC,” *Phys. Lett. B* **716** (2012) 1–29, [arXiv:1207.7214](https://arxiv.org/abs/1207.7214) [hep-ex].
- [2] **CMS** Collaboration, S. Chatrchyan *et al.*, “Observation of a New Boson at a Mass of 125 GeV with the CMS Experiment at the LHC,” *Phys. Lett. B* **716** (2012) 30–61, [arXiv:1207.7235](https://arxiv.org/abs/1207.7235) [hep-ex].
- [3] **ATLAS** Collaboration, G. Aad *et al.*, “A detailed map of Higgs boson interactions by the ATLAS experiment ten years after the discovery,” *Nature* **607** no. 7917, (2022) 52–59, [arXiv:2207.00092](https://arxiv.org/abs/2207.00092) [hep-ex]. [Erratum: *Nature* 612, E24 (2022)].
- [4] **CMS** Collaboration, A. Tumasyan *et al.*, “A portrait of the Higgs boson by the CMS experiment ten years after the discovery.,” *Nature* **607** no. 7917, (2022) 60–68, [arXiv:2207.00043](https://arxiv.org/abs/2207.00043) [hep-ex].
- [5] W. Buchmüller and D. Wyler, “Effective lagrangian analysis of new interactions and flavour conservation,” *Nuclear Physics B* **268** no. 3, (1986) 621–653.
- [6] B. Grzadkowski, M. Iskrzynski, M. Misiak, and J. Rosiek, “Dimension-Six Terms in the Standard Model Lagrangian,” *JHEP* **10** (2010) 085, [arXiv:1008.4884](https://arxiv.org/abs/1008.4884) [hep-ph].
- [7] R. Contino, M. Ghezzi, C. Grojean, M. Muhlleitner, and M. Spira, “Effective Lagrangian for a light Higgs-like scalar,” *JHEP* **07** (2013) 035, [arXiv:1303.3876](https://arxiv.org/abs/1303.3876) [hep-ph].
- [8] F. Feruglio, “The Chiral approach to the electroweak interactions,” *Int. J. Mod. Phys. A* **8** (1993) 4937–4972, [arXiv:hep-ph/9301281](https://arxiv.org/abs/hep-ph/9301281).
- [9] C. P. Burgess, J. Matias, and M. Pospelov, “A Higgs or not a Higgs? What to do if you discover a new scalar particle,” *Int. J. Mod. Phys. A* **17** (2002) 1841–1918, [arXiv:hep-ph/9912459](https://arxiv.org/abs/hep-ph/9912459).
- [10] R. Contino, C. Grojean, M. Moretti, F. Piccinini, and R. Rattazzi, “Strong Double Higgs Production at the LHC,” *JHEP* **05** (2010) 089, [arXiv:1002.1011](https://arxiv.org/abs/1002.1011) [hep-ph].
- [11] G. Buchalla and O. Cata, “Effective Theory of a Dynamically Broken Electroweak Standard Model at NLO,” *JHEP* **07** (2012) 101, [arXiv:1203.6510](https://arxiv.org/abs/1203.6510) [hep-ph].
- [12] R. Alonso, M. B. Gavela, L. Merlo, S. Rigolin, and J. Yépés, “The Effective Chiral Lagrangian for a Light Dynamical ”Higgs Particle”,” *Phys. Lett. B* **722** (2013) 330–335, [arXiv:1212.3305](https://arxiv.org/abs/1212.3305) [hep-ph]. [Erratum: *Phys.Lett.B* 726, 926 (2013)].
- [13] I. Brivio, T. Corbett, O. J. P. Éboli, M. B. Gavela, J. Gonzalez-Fraile, M. C. Gonzalez-Garcia, L. Merlo, and S. Rigolin, “Disentangling a dynamical Higgs,” *JHEP* **03** (2014) 024, [arXiv:1311.1823](https://arxiv.org/abs/1311.1823) [hep-ph].

- [14] G. Buchalla, O. Cata, A. Celis, and C. Krause, “Note on Anomalous Higgs-Boson Couplings in Effective Field Theory,” *Phys. Lett. B* **750** (2015) 298–301, [arXiv:1504.01707 \[hep-ph\]](https://arxiv.org/abs/1504.01707).
- [15] B. M. Gavela, E. E. Jenkins, A. V. Manohar, and L. Merlo, “Analysis of General Power Counting Rules in Effective Field Theory,” *Eur. Phys. J. C* **76** no. 9, (2016) 485, [arXiv:1601.07551 \[hep-ph\]](https://arxiv.org/abs/1601.07551).
- [16] G. Buchalla, O. Catá, and C. Krause, “On the Power Counting in Effective Field Theories,” *Phys. Lett. B* **731** (2014) 80–86, [arXiv:1312.5624 \[hep-ph\]](https://arxiv.org/abs/1312.5624).
- [17] I. Brivio, R. Gröber, and K. Schmid, “The Art of Counting: a reappraisal of the HEFT expansion,” [arXiv:2511.23410 \[hep-ph\]](https://arxiv.org/abs/2511.23410).
- [18] A. Falkowski and R. Rattazzi, “Which EFT,” *JHEP* **10** (2019) 255, [arXiv:1902.05936 \[hep-ph\]](https://arxiv.org/abs/1902.05936).
- [19] R. Alonso, E. E. Jenkins, and A. V. Manohar, “A Geometric Formulation of Higgs Effective Field Theory: Measuring the Curvature of Scalar Field Space,” *Phys. Lett. B* **754** (2016) 335–342, [arXiv:1511.00724 \[hep-ph\]](https://arxiv.org/abs/1511.00724).
- [20] R. Alonso, E. E. Jenkins, and A. V. Manohar, “Sigma Models with Negative Curvature,” *Phys. Lett. B* **756** (2016) 358–364, [arXiv:1602.00706 \[hep-ph\]](https://arxiv.org/abs/1602.00706).
- [21] R. Alonso, E. E. Jenkins, and A. V. Manohar, “Geometry of the Scalar Sector,” *JHEP* **08** (2016) 101, [arXiv:1605.03602 \[hep-ph\]](https://arxiv.org/abs/1605.03602).
- [22] T. Cohen, N. Craig, X. Lu, and D. Sutherland, “Is SMEFT Enough?,” *JHEP* **03** (2021) 237, [arXiv:2008.08597 \[hep-ph\]](https://arxiv.org/abs/2008.08597).
- [23] R. Gómez-Ambrosio, F. J. Llanes-Estrada, A. Salas-Bernárdez, and J. J. Sanz-Cillero, “Distinguishing electroweak EFTs with $W_L W_L \rightarrow n \times h$,” *Phys. Rev. D* **106** no. 5, (2022) 053004, [arXiv:2204.01763 \[hep-ph\]](https://arxiv.org/abs/2204.01763).
- [24] R. Gómez-Ambrosio, F. J. Llanes-Estrada, A. Salas-Bernárdez, and J. J. Sanz-Cillero, “SMEFT is falsifiable through multi-Higgs measurements (even in the absence of new light particles),” *Commun. Theor. Phys.* **75** no. 9, (2023) 095202, [arXiv:2207.09848 \[hep-ph\]](https://arxiv.org/abs/2207.09848).
- [25] I. Brivio and M. Trott, “The Standard Model as an Effective Field Theory,” *Phys. Rept.* **793** (2019) 1–98, [arXiv:1706.08945 \[hep-ph\]](https://arxiv.org/abs/1706.08945).
- [26] A. Djouadi, W. Kilian, M. Muhlleitner, and P. M. Zerwas, “Production of neutral Higgs boson pairs at LHC,” *Eur. Phys. J. C* **10** (1999) 45–49, [arXiv:hep-ph/9904287](https://arxiv.org/abs/hep-ph/9904287).
- [27] M. J. Dolan, C. Englert, and M. Spannowsky, “Higgs self-coupling measurements at the LHC,” *JHEP* **10** (2012) 112, [arXiv:1206.5001 \[hep-ph\]](https://arxiv.org/abs/1206.5001).

[28] J. Baglio, A. Djouadi, R. Gröber, M. M. Mühlleitner, J. Quevillon, and M. Spira, “The measurement of the Higgs self-coupling at the LHC: theoretical status,” *JHEP* **04** (2013) 151, [arXiv:1212.5581 \[hep-ph\]](https://arxiv.org/abs/1212.5581).

[29] R. Grober and M. Muhlleitner, “Composite Higgs Boson Pair Production at the LHC,” *JHEP* **06** (2011) 020, [arXiv:1012.1562 \[hep-ph\]](https://arxiv.org/abs/1012.1562).

[30] R. Contino, M. Ghezzi, M. Moretti, G. Panico, F. Piccinini, and A. Wulzer, “Anomalous Couplings in Double Higgs Production,” *JHEP* **08** (2012) 154, [arXiv:1205.5444 \[hep-ph\]](https://arxiv.org/abs/1205.5444).

[31] R. Grober, M. Muhlleitner, and M. Spira, “Signs of Composite Higgs Pair Production at Next-to-Leading Order,” *JHEP* **06** (2016) 080, [arXiv:1602.05851 \[hep-ph\]](https://arxiv.org/abs/1602.05851).

[32] R. L. Delgado, R. Gómez-Ambrosio, J. Martínez-Martín, A. Salas-Bernárdez, and J. J. Sanz-Cillero, “Production of two, three, and four Higgs bosons: where SMEFT and HEFT depart,” *JHEP* **03** (2024) 037, [arXiv:2311.04280 \[hep-ph\]](https://arxiv.org/abs/2311.04280).

[33] R. Gröber, A. N. Rossia, and M. Ryczkowski, “Multi-Higgs Amplitudes Bootstrapped: Dissecting SMEFT and HEFT,” [arXiv:2509.02680 \[hep-ph\]](https://arxiv.org/abs/2509.02680).

[34] CMS Collaboration, A. Tumasyan *et al.*, “Search for Nonresonant Pair Production of Highly Energetic Higgs Bosons Decaying to Bottom Quarks,” *Phys. Rev. Lett.* **131** no. 4, (2023) 041803, [arXiv:2205.06667 \[hep-ex\]](https://arxiv.org/abs/2205.06667).

[35] ATLAS Collaboration, “HEFT interpretations of Higgs boson pair searches in $b\bar{b}\gamma\gamma$ and $b\bar{b}\tau\tau$ final states and of their combination in ATLAS,” ATL-PHYS-PUB-2022-019.

[36] I. Banta, T. Cohen, N. Craig, X. Lu, and D. Sutherland, “Non-decoupling new particles,” *JHEP* **02** (2022) 029, [arXiv:2110.02967 \[hep-ph\]](https://arxiv.org/abs/2110.02967).

[37] G. Crawford and D. Sutherland, “Scalars with non-decoupling phenomenology at future colliders,” *JHEP* **04** (2025) 197, [arXiv:2409.18177 \[hep-ph\]](https://arxiv.org/abs/2409.18177).

[38] C. Kilic, S. Mathai, and T. Youn, “Constraints on Loryons in a Two Higgs Doublet Model,” [arXiv:2601.14389 \[hep-ph\]](https://arxiv.org/abs/2601.14389).

[39] C. Englert, W. Naskar, and D. Sutherland, “BSM patterns in scalar-sector coupling modifiers,” *JHEP* **11** (2023) 158, [arXiv:2307.14809 \[hep-ph\]](https://arxiv.org/abs/2307.14809).

[40] S. Dawson, S. Dittmaier, and M. Spira, “Neutral Higgs boson pair production at hadron colliders: QCD corrections,” *Phys. Rev. D* **58** (1998) 115012, [arXiv:hep-ph/9805244](https://arxiv.org/abs/hep-ph/9805244).

[41] J. Baglio, F. Campanario, S. Glaus, M. Mühlleitner, M. Spira, and J. Streicher, “Gluon fusion into Higgs pairs at NLO QCD and the top mass scheme,” *Eur. Phys. J. C* **79** no. 6, (2019) 459, [arXiv:1811.05692 \[hep-ph\]](https://arxiv.org/abs/1811.05692).

- [42] S. Borowka, N. Greiner, G. Heinrich, S. P. Jones, M. Kerner, J. Schlenk, U. Schubert, and T. Zirke, “Higgs Boson Pair Production in Gluon Fusion at Next-to-Leading Order with Full Top-Quark Mass Dependence,” *Phys. Rev. Lett.* **117** no. 1, (2016) 012001, [arXiv:1604.06447 \[hep-ph\]](https://arxiv.org/abs/1604.06447). [Erratum: Phys.Rev.Lett. 117, 079901 (2016)].
- [43] S. Borowka, N. Greiner, G. Heinrich, S. P. Jones, M. Kerner, J. Schlenk, and T. Zirke, “Full top quark mass dependence in Higgs boson pair production at NLO,” *JHEP* **10** (2016) 107, [arXiv:1608.04798 \[hep-ph\]](https://arxiv.org/abs/1608.04798).
- [44] M. Grazzini, G. Heinrich, S. Jones, S. Kallweit, M. Kerner, J. M. Lindert, and J. Mazzitelli, “Higgs boson pair production at NNLO with top quark mass effects,” *JHEP* **05** (2018) 059, [arXiv:1803.02463 \[hep-ph\]](https://arxiv.org/abs/1803.02463).
- [45] A. A H and H.-S. Shao, “N³LO+N³LL QCD improved Higgs pair cross sections,” *JHEP* **02** (2023) 067, [arXiv:2209.03914 \[hep-ph\]](https://arxiv.org/abs/2209.03914).
- [46] E. Bagnaschi, G. Degrassi, and R. Gröber, “Higgs boson pair production at NLO in the POWHEG approach and the top quark mass uncertainties,” *Eur. Phys. J. C* **83** no. 11, (2023) 1054, [arXiv:2309.10525 \[hep-ph\]](https://arxiv.org/abs/2309.10525).
- [47] L. S. Ling, R. Y. Zhang, W.-G. Ma, L. Guo, W. H. Li, and X. Z. Li, “NNLO QCD corrections to Higgs pair production via vector boson fusion at hadron colliders,” *Phys. Rev. D* **89** no. 7, (2014) 073001, [arXiv:1401.7754 \[hep-ph\]](https://arxiv.org/abs/1401.7754).
- [48] F. A. Dreyer and A. Karlberg, “Vector-Boson Fusion Higgs Pair Production at N³LO,” *Phys. Rev. D* **98** no. 11, (2018) 114016, [arXiv:1811.07906 \[hep-ph\]](https://arxiv.org/abs/1811.07906).
- [49] F. A. Dreyer, A. Karlberg, J.-N. Lang, and M. Pellen, “Precise predictions for double-Higgs production via vector-boson fusion,” *Eur. Phys. J. C* **80** no. 11, (2020) 1037, [arXiv:2005.13341 \[hep-ph\]](https://arxiv.org/abs/2005.13341).
- [50] L. Alasfar, R. Corral Lopez, and R. Gröber, “Probing Higgs couplings to light quarks via Higgs pair production,” *JHEP* **11** (2019) 088, [arXiv:1909.05279 \[hep-ph\]](https://arxiv.org/abs/1909.05279).
- [51] L. Alasfar, R. Gröber, C. Grojean, A. Paul, and Z. Qian, “Machine learning the trilinear and light-quark Yukawa couplings from Higgs pair kinematic shapes,” *JHEP* **11** (2022) 045, [arXiv:2207.04157 \[hep-ph\]](https://arxiv.org/abs/2207.04157).
- [52] E. Celada, T. Han, W. Kilian, N. Kreher, Y. Ma, F. Maltoni, D. Pagani, J. Reuter, T. Striegl, and K. Xie, “Probing Higgs-muon interactions at a multi-TeV muon collider,” *JHEP* **08** (2024) 021, [arXiv:2312.13082 \[hep-ph\]](https://arxiv.org/abs/2312.13082).
- [53] T. Han, D. Liu, I. Low, and X. Wang, “Electroweak scattering at the muon shot,” *Phys. Rev. D* **110** no. 1, (2024) 013005, [arXiv:2312.07670 \[hep-ph\]](https://arxiv.org/abs/2312.07670).
- [54] R. Grober, M. Muhlleitner, and M. Spira, “Higgs Pair Production at NLO QCD for CP-violating Higgs Sectors,” *Nucl. Phys. B* **925** (2017) 1–27, [arXiv:1705.05314 \[hep-ph\]](https://arxiv.org/abs/1705.05314).

[55] C. Arzt, M. B. Einhorn, and J. Wudka, “Patterns of deviation from the standard model,” *Nucl. Phys. B* **433** (1995) 41–66, [arXiv:hep-ph/9405214](https://arxiv.org/abs/hep-ph/9405214).

[56] G. Buchalla, G. Heinrich, C. Müller-Salditt, and F. Pandler, “Loop counting matters in SMEFT,” *SciPost Phys.* **15** no. 3, (2023) 088, [arXiv:2204.11808](https://arxiv.org/abs/2204.11808) [hep-ph].

[57] S. Di Noi, R. Gröber, G. Heinrich, J. Lang, and M. Vitti, “ $\gamma 5$ schemes and the interplay of SMEFT operators in the Higgs-gluon coupling,” *Phys. Rev. D* **109** no. 9, (2024) 095024, [arXiv:2310.18221](https://arxiv.org/abs/2310.18221) [hep-ph].

[58] G. Heinrich and J. Lang, “Combining chromomagnetic and four-fermion operators with leading SMEFT operators for $gg \rightarrow hh$ at NLO QCD,” *JHEP* **05** (2024) 121, [arXiv:2311.15004](https://arxiv.org/abs/2311.15004) [hep-ph].

[59] L. Alasfar *et al.*, “Effective Field Theory descriptions of Higgs boson pair production,” *SciPost Phys. Comm. Rep.* **2024** (2024) 2, [arXiv:2304.01968](https://arxiv.org/abs/2304.01968) [hep-ph].

[60] I. Brivio, R. Gröber, and K. Schmid, “Higgs pair production in gluon fusion to higher orders in Higgs Effective Field Theory,” [arXiv:2511.23411](https://arxiv.org/abs/2511.23411) [hep-ph].

[61] I. Brivio, R. Gröber, K. Mimasu, and K. Schmid, “Di-higgs production from gluon fusion at dimension-8 in smeft.” To appear.

[62] A. Dedes, J. Rosiek, and M. Ryczkowski, “Double Higgs boson production via vector boson fusion in SMEFT,” *Phys. Rev. D* **112** no. 5, (2025) 055044, [arXiv:2506.12917](https://arxiv.org/abs/2506.12917) [hep-ph].

[63] M. J. Herrero and R. A. Morales, “One-loop corrections for WW to HH in Higgs EFT with the electroweak chiral Lagrangian,” *Phys. Rev. D* **106** no. 7, (2022) 073008, [arXiv:2208.05900](https://arxiv.org/abs/2208.05900) [hep-ph].

[64] F. Arco, D. Domenech, M. J. Herrero, and R. A. Morales, “Nondecoupling effects from heavy Higgs bosons by matching 2HDM to HEFT amplitudes,” *Phys. Rev. D* **108** no. 9, (2023) 095013, [arXiv:2307.15693](https://arxiv.org/abs/2307.15693) [hep-ph].

[65] L. Di Luzio, R. Gröber, and M. Spannowsky, “Maxi-sizing the trilinear Higgs self-coupling: how large could it be?,” *Eur. Phys. J. C* **77** no. 11, (2017) 788, [arXiv:1704.02311](https://arxiv.org/abs/1704.02311) [hep-ph].

[66] B. W. Lee, C. Quigg, and H. B. Thacker, “Weak interactions at very high energies: The role of the higgs-boson mass,” *Phys. Rev. D* **16** (Sep, 1977) 1519–1531. <https://link.aps.org/doi/10.1103/PhysRevD.16.1519>.

[67] M. D. Goodsell and F. Staub, “Unitarity constraints on general scalar couplings with SARAH,” *Eur. Phys. J. C* **78** no. 8, (2018) 649, [arXiv:1805.07306](https://arxiv.org/abs/1805.07306) [hep-ph].

[68] D. López-Val and T. Robens, “ Δr and the W-boson mass in the singlet extension of the standard model,” *Phys. Rev. D* **90** (2014) 114018, [arXiv:1406.1043](https://arxiv.org/abs/1406.1043) [hep-ph].

[69] A. Papaefstathiou, T. Robens, and G. White, “Signal strength and W-boson mass measurements as a probe of the electro-weak phase transition at colliders - Snowmass White Paper,” in *Snowmass 2021*. 5, 2022. [arXiv:2205.14379 \[hep-ph\]](https://arxiv.org/abs/2205.14379).

[70] **ATLAS** Collaboration, G. Aad *et al.*, “Measurement of the W-boson mass and width with the ATLAS detector using proton–proton collisions at $\sqrt{s} = 7$ TeV,” *Eur. Phys. J. C* **84** no. 12, (2024) 1309, [arXiv:2403.15085 \[hep-ex\]](https://arxiv.org/abs/2403.15085).

[71] **CMS** Collaboration, V. Chekhovsky *et al.*, “High-precision measurement of the W boson mass with the CMS experiment at the LHC,” [arXiv:2412.13872 \[hep-ex\]](https://arxiv.org/abs/2412.13872).

[72] J. de Blas, J. C. Criado, M. Perez-Victoria, and J. Santiago, “Effective description of general extensions of the Standard Model: the complete tree-level dictionary,” *JHEP* **03** (2018) 109, [arXiv:1711.10391 \[hep-ph\]](https://arxiv.org/abs/1711.10391).

[73] M. Jiang, N. Craig, Y.-Y. Li, and D. Sutherland, “Complete one-loop matching for a singlet scalar in the Standard Model EFT,” *JHEP* **02** (2019) 031, [arXiv:1811.08878 \[hep-ph\]](https://arxiv.org/abs/1811.08878). [Erratum: JHEP 01, 135 (2021)].

[74] U. Haisch, M. Ruhdorfer, E. Salvioni, E. Venturini, and A. Weiler, “Singlet night in Feynman-ville: one-loop matching of a real scalar,” *JHEP* **04** (2020) 164, [arXiv:2003.05936 \[hep-ph\]](https://arxiv.org/abs/2003.05936). [Erratum: JHEP 07, 066 (2020)].

[75] S. Dawson, D. Fontes, C. Quezada-Calonge, and J. J. Sanz-Cillero, “Is the HEFT matching unique?,” *Phys. Rev. D* **109** no. 5, (2024) 055037, [arXiv:2311.16897 \[hep-ph\]](https://arxiv.org/abs/2311.16897).

[76] S. Dawson, S. Homiller, and S. D. Lane, “Putting standard model EFT fits to work,” *Phys. Rev. D* **102** no. 5, (2020) 055012, [arXiv:2007.01296 \[hep-ph\]](https://arxiv.org/abs/2007.01296).

[77] Z. Ge, H. Song, and X. Wan, “Establishing the Primary HEFT as a Precision Benchmark for UV-HEFT Matching,” [arXiv:2602.14418 \[hep-ph\]](https://arxiv.org/abs/2602.14418).

[78] S. Dittmaier, S. Schuhmacher, and M. Stahlhofen, “Integrating out heavy fields in the path integral using the background-field method: general formalism,” *Eur. Phys. J. C* **81** no. 9, (2021) 826, [arXiv:2102.12020 \[hep-ph\]](https://arxiv.org/abs/2102.12020).

[79] G. Buchalla, O. Cata, A. Celis, and C. Krause, “Standard Model Extended by a Heavy Singlet: Linear vs. Nonlinear EFT,” *Nucl. Phys. B* **917** (2017) 209–233, [arXiv:1608.03564 \[hep-ph\]](https://arxiv.org/abs/1608.03564).

[80] Michael Spira, “hpair.” <https://https://ltpth.pages.psi.ch/tiger/>. Accessed: 2026-01-15.

[81] R. Grober, M. Muhlleitner, M. Spira, and J. Streicher, “NLO QCD Corrections to Higgs Pair Production including Dimension-6 Operators,” *JHEP* **09** (2015) 092, [arXiv:1504.06577 \[hep-ph\]](https://arxiv.org/abs/1504.06577).

[82] G. Buchalla, M. Capozi, A. Celis, G. Heinrich, and L. Scyboz, “Higgs boson pair production in non-linear Effective Field Theory with full m_t -dependence at NLO QCD,” *JHEP* **09** (2018) 057, [arXiv:1806.05162 \[hep-ph\]](https://arxiv.org/abs/1806.05162). [Erratum: JHEP 06, 094 (2025)].

[83] G. Heinrich, J. Lang, and L. Scyboz, “SMEFT predictions for $gg \rightarrow hh$ at full NLO QCD and truncation uncertainties,” *JHEP* **08** (2022) 079, [arXiv:2204.13045 \[hep-ph\]](https://arxiv.org/abs/2204.13045). [Erratum: JHEP 10, 086 (2023)].

[84] A. Djouadi, J. Kalinowski, and M. Spira, “HDECAY: A Program for Higgs boson decays in the standard model and its supersymmetric extension,” *Comput. Phys. Commun.* **108** (1998) 56–74, [arXiv:hep-ph/9704448](https://arxiv.org/abs/hep-ph/9704448).

[85] **HDECAY** Collaboration, A. Djouadi, J. Kalinowski, M. Muehlleitner, and M. Spira, “HDECAY: Twenty₊₊ years after,” *Comput. Phys. Commun.* **238** (2019) 214–231, [arXiv:1801.09506 \[hep-ph\]](https://arxiv.org/abs/1801.09506).

[86] G. Heinrich, J. Lang, and L. Scyboz, “Beyond dimension six in SM Effective Field Theory: a case study in Higgs pair production at NLO QCD,” *PoS LL2022* (2022) 009, [arXiv:2207.08790 \[hep-ph\]](https://arxiv.org/abs/2207.08790).

[87] H. Song and X. Wan, “Matching the real Higgs triplet extension of Standard Model to HEFT,” *JHEP* **06** (2025) 249, [arXiv:2503.00707 \[hep-ph\]](https://arxiv.org/abs/2503.00707).

[88] J. Braun, P. Bredt, G. Heinrich, and M. Höfer, “Double Higgs production in vector boson fusion at NLO QCD in HEFT,” *JHEP* **07** (2025) 209, [arXiv:2502.09132 \[hep-ph\]](https://arxiv.org/abs/2502.09132).

[89] B. Jäger, A. Karlberg, and S. Reinhardt, “Precision tools for the simulation of double-Higgs production via vector-boson fusion,” *JHEP* **06** (2025) 022, [arXiv:2502.09112 \[hep-ph\]](https://arxiv.org/abs/2502.09112).

[90] G. C. Branco, P. M. Ferreira, L. Lavoura, M. N. Rebelo, M. Sher, and J. P. Silva, “Theory and phenomenology of two-Higgs-doublet models,” *Phys. Rept.* **516** (2012) 1–102, [arXiv:1106.0034 \[hep-ph\]](https://arxiv.org/abs/1106.0034).

[91] S. Davidson and H. E. Haber, “Basis-independent methods for the two-Higgs-doublet model,” *Phys. Rev. D* **72** (2005) 035004, [arXiv:hep-ph/0504050](https://arxiv.org/abs/hep-ph/0504050). [Erratum: Phys. Rev. D 72, 099902 (2005)].

[92] G. Degrassi and P. Slavich, “On the two-loop BSM corrections to $h \rightarrow \gamma\gamma$ in the aligned THDM,” *Eur. Phys. J. C* **83** no. 10, (2023) 941, [arXiv:2307.02476 \[hep-ph\]](https://arxiv.org/abs/2307.02476).

[93] S. Dawson, D. Fontes, S. Homiller, and M. Sullivan, “Role of dimension-eight operators in an EFT for the 2HDM,” *Phys. Rev. D* **106** no. 5, (2022) 055012, [arXiv:2205.01561 \[hep-ph\]](https://arxiv.org/abs/2205.01561).

[94] S. Das Bakshi, S. Dawson, D. Fontes, and S. Homiller, “Relevance of one-loop SMEFT matching in the 2HDM,” *Phys. Rev. D* **109** no. 7, (2024) 075022, [arXiv:2401.12279 \[hep-ph\]](https://arxiv.org/abs/2401.12279).

[95] I. Banta, T. Cohen, N. Craig, X. Lu, and D. Sutherland, “Effective field theory of the two Higgs doublet model,” *JHEP* **06** (2023) 150, [arXiv:2304.09884 \[hep-ph\]](https://arxiv.org/abs/2304.09884).

[96] F. Arco, S. Heinemeyer, and M. J. Herrero, “Exploring sizable triple Higgs couplings in the 2HDM,” *Eur. Phys. J. C* **80** no. 9, (2020) 884, [arXiv:2005.10576 \[hep-ph\]](https://arxiv.org/abs/2005.10576).

[97] **ATLAS** Collaboration, G. Aad *et al.*, “Interpretations of the ATLAS measurements of Higgs boson production and decay rates and differential cross-sections in pp collisions at $\sqrt{s} = 13$ TeV,” *JHEP* **11** (2024) 097, [arXiv:2402.05742 \[hep-ex\]](https://arxiv.org/abs/2402.05742).

[98] S. Kanemura, S. Kiyoura, Y. Okada, E. Senaha, and C. P. Yuan, “New physics effect on the Higgs selfcoupling,” *Phys. Lett. B* **558** (2003) 157–164, [arXiv:hep-ph/0211308](https://arxiv.org/abs/hep-ph/0211308).

[99] S. Kanemura, Y. Okada, E. Senaha, and C. P. Yuan, “Higgs coupling constants as a probe of new physics,” *Phys. Rev. D* **70** (2004) 115002, [arXiv:hep-ph/0408364](https://arxiv.org/abs/hep-ph/0408364).

[100] J. Braathen and S. Kanemura, “On two-loop corrections to the Higgs trilinear coupling in models with extended scalar sectors,” *Phys. Lett. B* **796** (2019) 38–46, [arXiv:1903.05417 \[hep-ph\]](https://arxiv.org/abs/1903.05417).

[101] J. Braathen and S. Kanemura, “Leading two-loop corrections to the Higgs boson self-couplings in models with extended scalar sectors,” *Eur. Phys. J. C* **80** no. 3, (2020) 227, [arXiv:1911.11507 \[hep-ph\]](https://arxiv.org/abs/1911.11507).

[102] H. Bahl, J. Braathen, M. Gabelmann, and G. Weiglein, “anyH3: precise predictions for the trilinear Higgs coupling in the Standard Model and beyond,” *Eur. Phys. J. C* **83** no. 12, (2023) 1156, [arXiv:2305.03015 \[hep-ph\]](https://arxiv.org/abs/2305.03015). [Erratum: Eur.Phys.J.C 84, 498 (2024)].

[103] G. Degrassi, R. Gröber, and P. Slavich, “Two-loop BSM contributions to Higgs pair production in the aligned THDM,” *JHEP* **01** (2026) 041, [arXiv:2508.11539 \[hep-ph\]](https://arxiv.org/abs/2508.11539).

[104] I. Brivio, “SMEFTsim 3.0 — a practical guide,” *JHEP* **04** (2021) 073, [arXiv:2012.11343 \[hep-ph\]](https://arxiv.org/abs/2012.11343).

[105] J. Fuentes-Martín, M. König, J. Pagès, A. E. Thomsen, and F. Wilsch, “A proof of concept for matchete: an automated tool for matching effective theories,” *Eur. Phys. J. C* **83** no. 7, (2023) 662, [arXiv:2212.04510 \[hep-ph\]](https://arxiv.org/abs/2212.04510).

[106] A. Pierce, J. Thaler, and L.-T. Wang, “Disentangling Dimension Six Operators through Di-Higgs Boson Production,” *JHEP* **05** (2007) 070, [arXiv:hep-ph/0609049](https://arxiv.org/abs/hep-ph/0609049).

- [107] J. Alison *et al.*, “Higgs boson potential at colliders: Status and perspectives,” *Rev. Phys.* **5** (2020) 100045, [arXiv:1910.00012 \[hep-ph\]](https://arxiv.org/abs/1910.00012).
- [108] F. Arco, S. Heinemeyer, and M. Mühlleitner, “Large one-loop effects of BSM triple Higgs couplings on double Higgs production at e^+e^- colliders,” *JHEP* **01** (2026) 160, [arXiv:2505.02947 \[hep-ph\]](https://arxiv.org/abs/2505.02947).
- [109] A. Alloul, N. D. Christensen, C. Degrande, C. Duhr, and B. Fuks, “FeynRules 2.0 - A complete toolbox for tree-level phenomenology,” *Comput. Phys. Commun.* **185** (2014) 2250–2300, [arXiv:1310.1921 \[hep-ph\]](https://arxiv.org/abs/1310.1921).